FACETS OF HEAVY-ION REACTIONS AROUND THE COULOMB BARRIER

Arshiya Sood
Post- Doctoral Research Associate
DeSiS – IPHC
arshiya.sood@iphc.cnrs.fr

RESEARCH EXPERIENCE

- **2015 – 2020 Doctor of Philosophy**

  Experimental Nuclear Physics - Low energy nuclear reactions
  Senior Research fellow (CGPA- 8.8/10.0)
  Director's Research Fellow (post-thesis submission)
  NuStaR lab, Department of Physics, Indian Institute of Technology Ropar

- **2021 – 2022 Post-doctoral research associate**

  Experimental Nuclear Physics - Nuclear Spectroscopy
  Nuclear Physics Division, KTH- The Royal Institute of Technology, Stockholm

- **2022 – Post-doctoral research associate**

  Measurement and simulations of secondary particles for ion-beam therapy and space radiation measurements.
  DeSIs-team, CNRS-IPHC, Strasbourg
  Supervision: Dr. Marie Vanstalle and Dr. Nicolas Arbor

Indian Institute of Technology Ropar, India

अंतर विश्वविद्यालय त्वरक केंद्र
Inter-University Accelerator Centre - (IUAC)

KTH- Royal Institute of Technology, Sweden

GSI Helmholtz Center for Heavy Ion Research · FAIR - Facility for Antiproton and Ion Research, Germany

Accelerator laboratory, University of Jvyäskylä, Finland

RESEARCH MOTIVATION

Heavy-Ion fusion reactions

- → nuclear astrophysics
- → energy generation in the stellar environment
- → production of exotic nuclei
- → synthesis of SHE
- → data to reach optimized irradiation conditions for the development of next generation nuclear reactors

Heavy-Ion peripheral reactions

- → QEL – potential parameters for different nuclear reactions
- → ICF and transfer - a promising spectroscopic tool to achieve high spin states
- → provide a sensitive probe for nuclear structure studies

Three sets of experiments were performed at Inter-University Accelerator Centre (IUAC), New Delhi

15UD PELLETRON @ IUAC

RESEARCH OUTLINE

Basics Introduction - Heavy-Ion Reactions

Expt. 01 Fission-like events in $^{12}C+^{169}Tm$ system at low excitation energies

Expt. 02 Reaction dependent entry state population: the case of $^{12}C+^{169}Tm$

Expt. 03 Quasi-elastic backscattering in $^{6,7}Li+^{116,118}Sn$ systems

Conclusion Summary and future perspectives

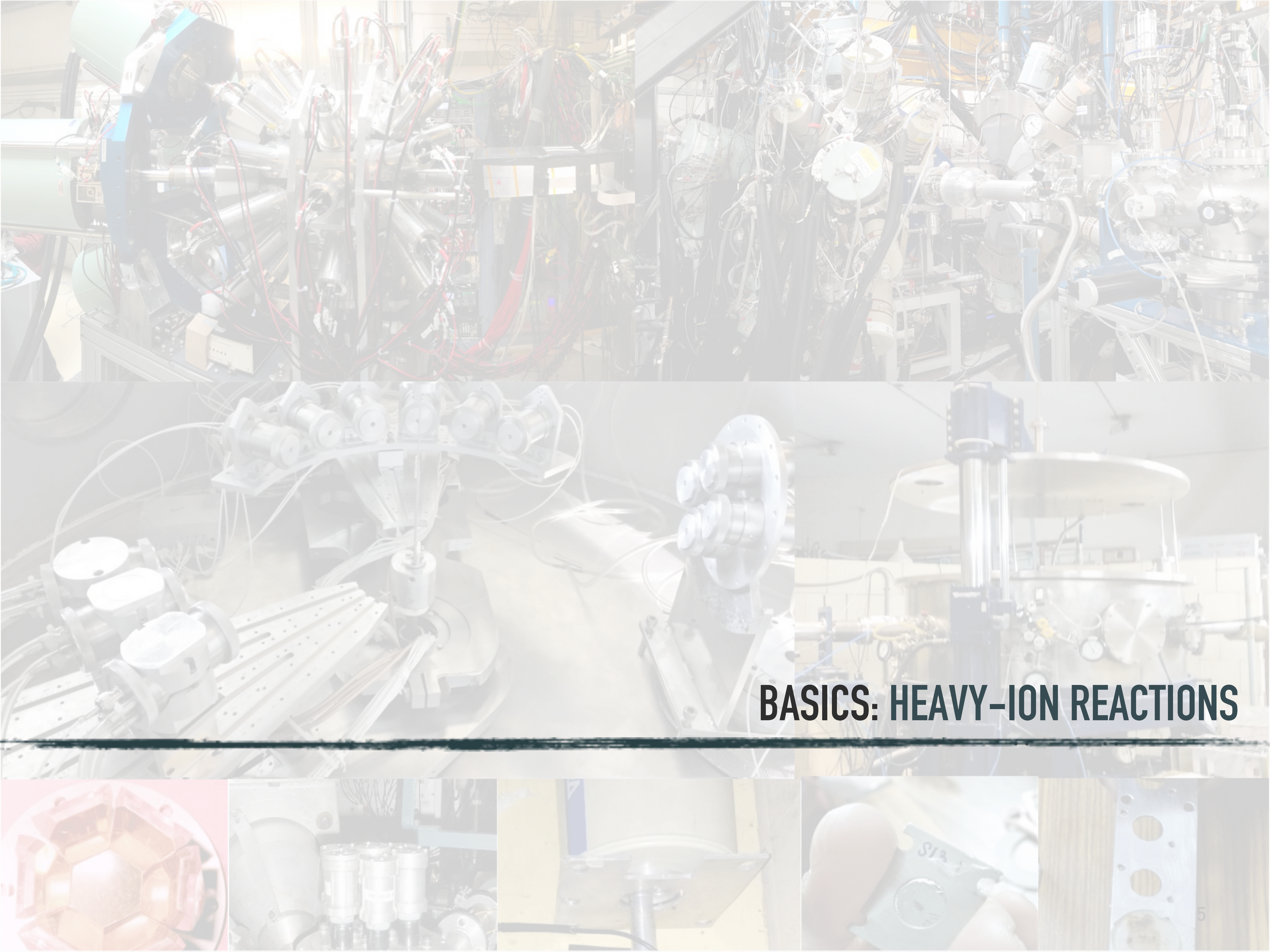

BASICS: HEAVY-ION REACTIONS

HEAVY-ION REACTIONS

Heavy-Ion reactions

Entrance channel **Exit channel**

Q-value

$$Q = (m_P + m_T - m_Y - m_b)c^2$$

Q < 0 → Endoergic, Q > 0 → Exoergic

Threshold energy

$$E_{th} \geq -Q(m_P + m_T)/m_T$$

Features

- **Transfer of cluster of nucleons and large angular momentum**
- **Small de-Broglie wavelength → semi-classical approach**

$$\lambda = \frac{1}{2\pi}\left[\frac{h^2}{2mE_{lab}}\right]^{1/2}$$

- **Semi-classical nature → description in terms of impact parameter**

Classification of Nuclear Reactions on the basis of impact parameter

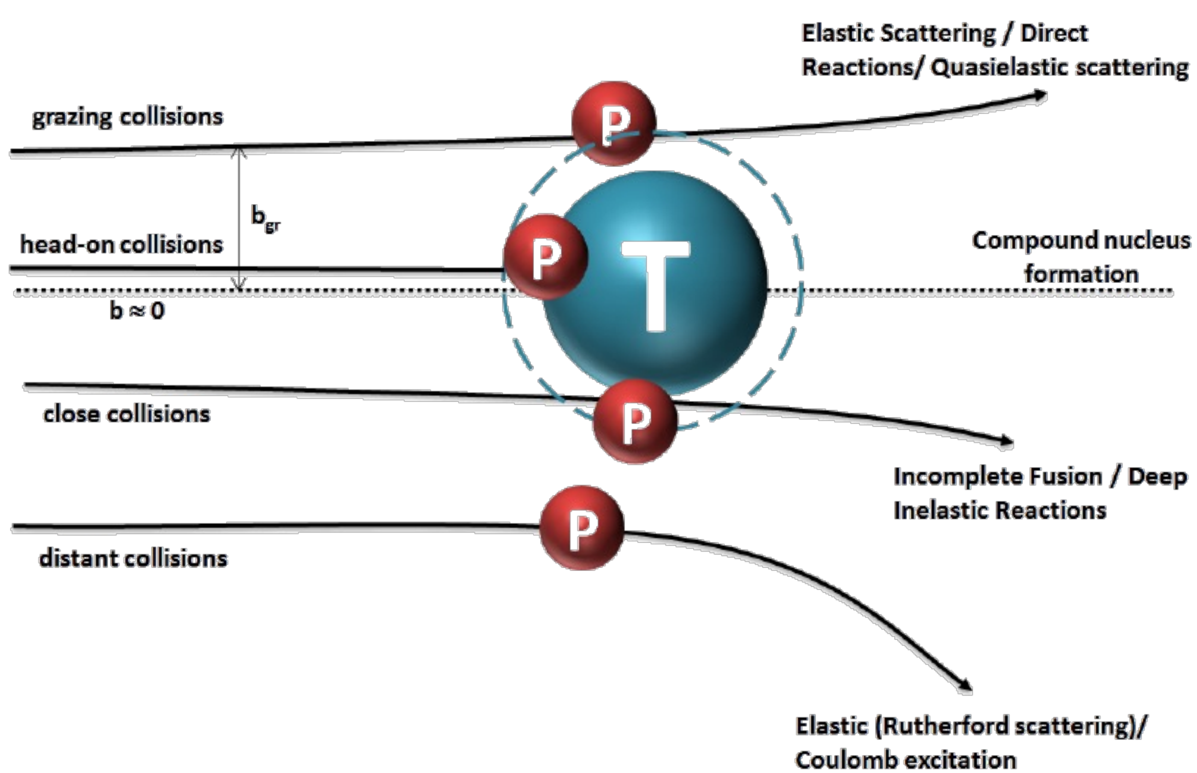

$$r_{min} = \frac{b}{\sqrt{1 - \frac{V(r_{min})}{E_{cm}}}}$$

b → Impact parameter

r_{min} → Distance of closest approach (= $R_P + R_T$)

HEAVY-ION REACTIONS

Classification on the basis of ℓ

Orbital angular momentum :

$$\ell/\hbar = (b\sqrt{2mE_{cm}})/\hbar = bk$$

Reaction x-section :

$$\sigma_R(\ell) = (2\ell+1)\pi\lambda\!\!\!^{-2}$$

Partial reaction x-sections :

$$\frac{d\sigma}{d\ell} = 2\pi\lambda\!\!\!^{-2}\ell$$

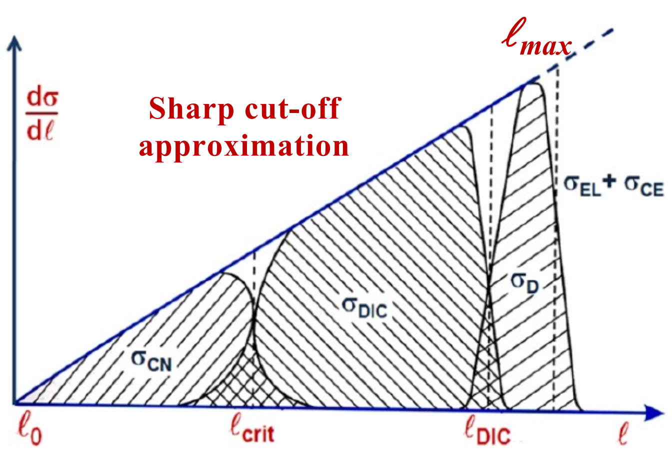

ICF characteristics

- **Fractional linear momentum transfer**
- $0 \leq \ell \leq \ell_{crit} \rightarrow CF;\ \ell_{crit} \leq \ell \leq \ell_{max} \rightarrow ICF$
- **Forward peaked PLFs**

$$E_{ejectile} = E_{projectile} \times {M_{ejectile}}/{M_{projectile}}$$

Interaction Potential

$$V_{eff}(r,\ell) = V_{Coul}(r) + V_{nucl}(r) + V_{cent}(r,\ell) = V(r) + V_{cent}(r,\ell)$$

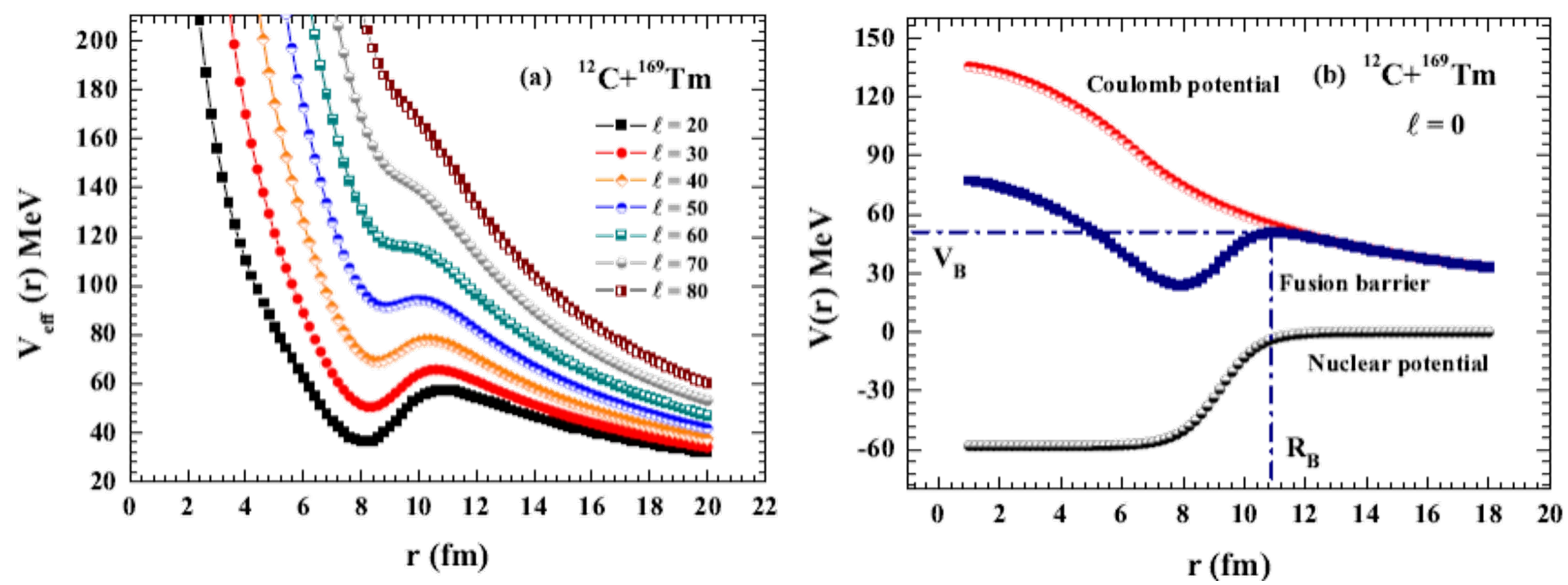

De-excitation of CN

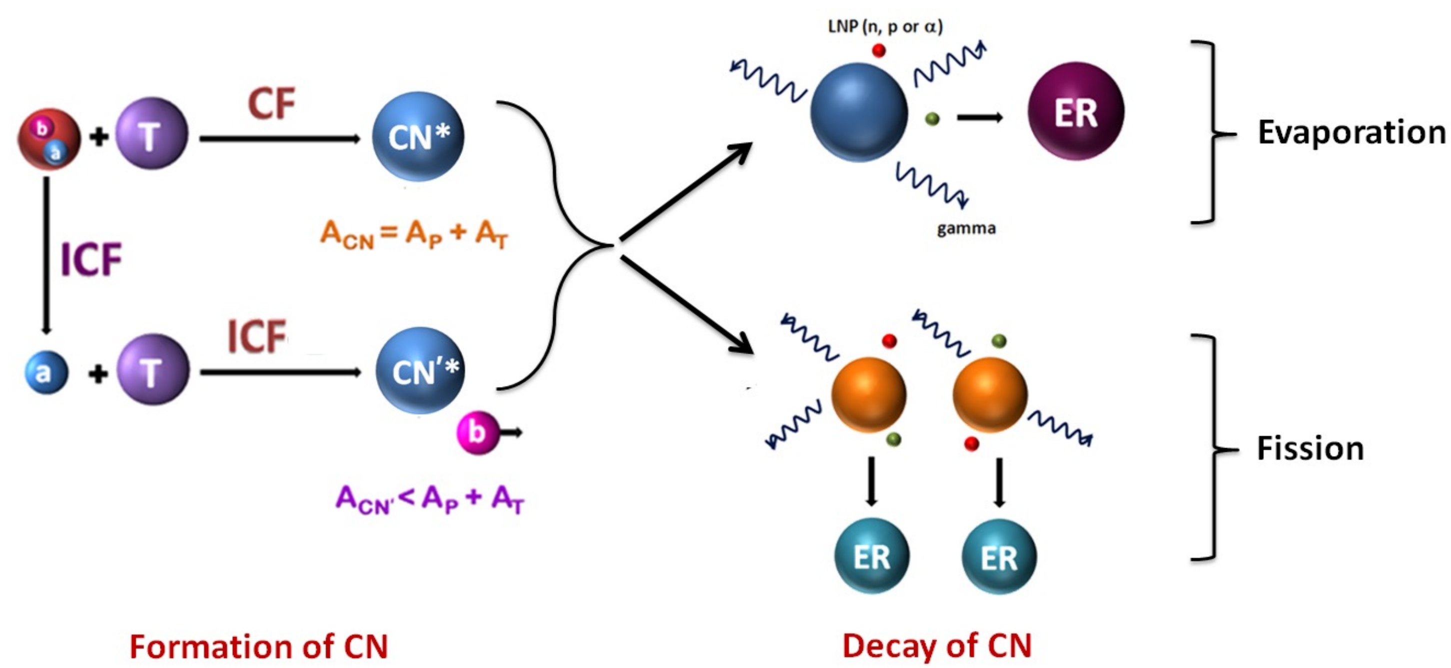

(Fusion- fission process)

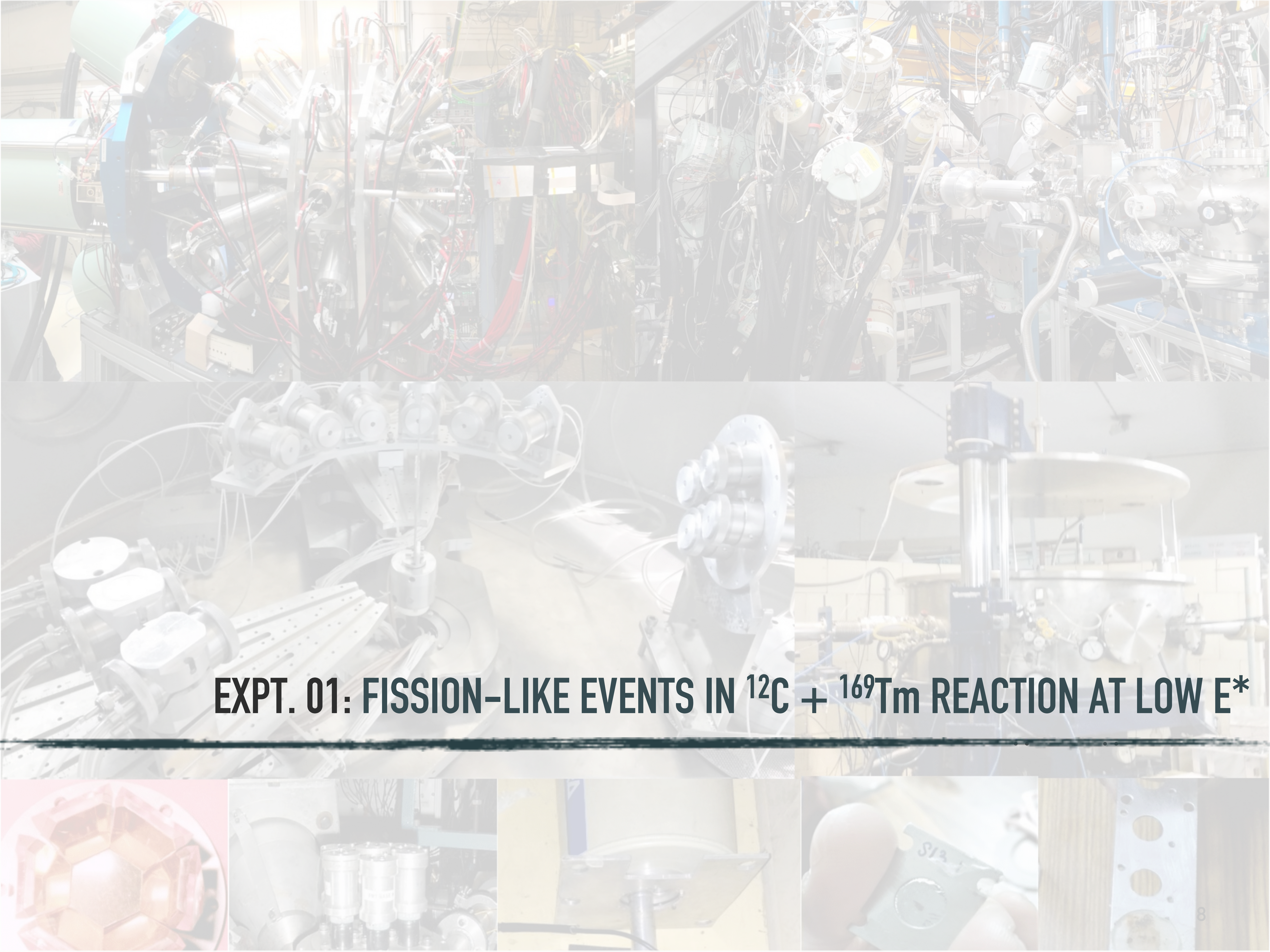

EXPT. 01: FISSION-LIKE EVENTS IN $^{12}C + ^{169}Tm$ REACTION AT LOW E*

FISSION-LIKE EVENTS IN $^{12}C + {}^{169}Tm$ REACTION AT LOW E*

Arshiya Sood et al., Physical Review C 96, 014620 (2017); Arshiya Sood et al., Acta Physica Polonica B 50, 291 (2019)

Motivation

- **Fission → dominant mode of de-excitation for HI induced reactions on actinide targets at high E*.**

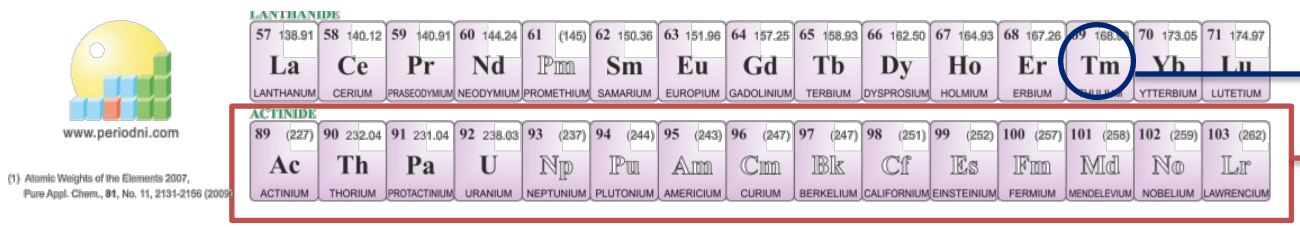

- **Paucity of studies and understanding of underlying dynamics → below actinide region and low excitation energies.**
- **The fusion-fission dynamics is influenced by various entrance channel parameters → excitation energy, mass-asymmetry, and deformation.**

Irradiation and offline spectroscopy

Experiment : **IUAC – GPSC beamline**

Facility : **General Purpose Scattering Chamber (GPSC)**

System : $^{12}C + {}^{169}Tm$

Detector : **High Purity Germanium Detectors (HPGe)**

Technique :
1. **Recoil-catcher activation and offline γ-ray spectroscopy.**
2. **Residue identification → characteristic γ-rays & decay-curve analysis**

E_{lab} : **77.18, 83.22, and 89.25 MeV**

E^* : **57, 63, and 69 MeV**

GPSC @ IUAC

Target-catcher stack

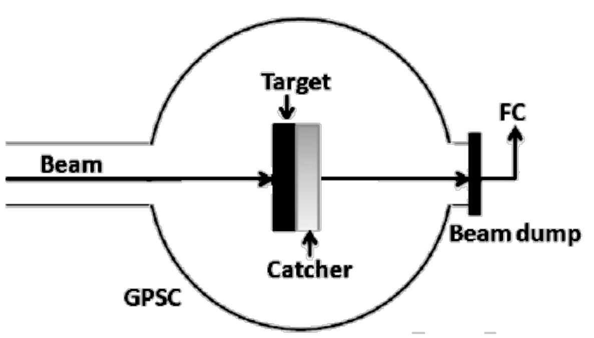

Counting set-up

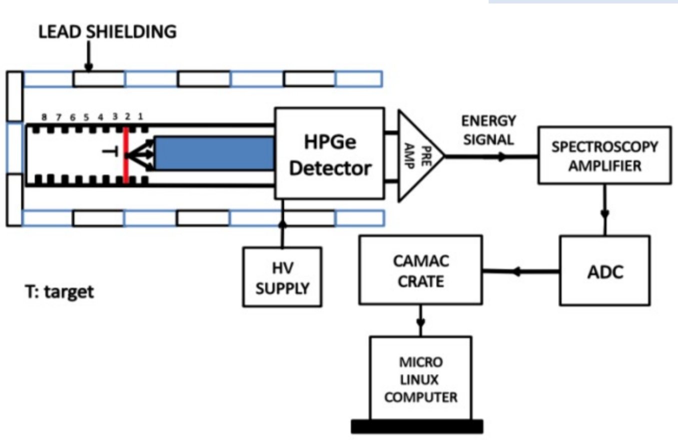

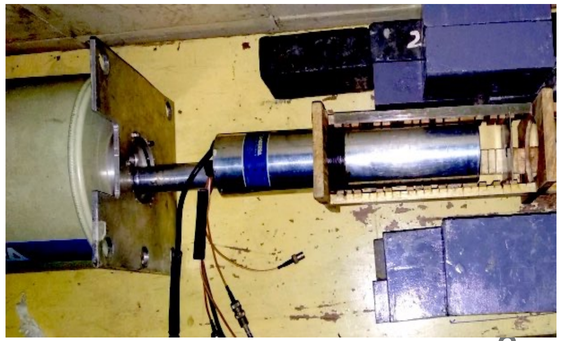

FISSION-LIKE EVENTS IN ^{12}C + ^{169}Tm REACTION AT LOW E*

Residue Identification – characteristic gamma rays & decay curve

Gamma-ray spectrum @ E_{lab}= 89.25 MeV

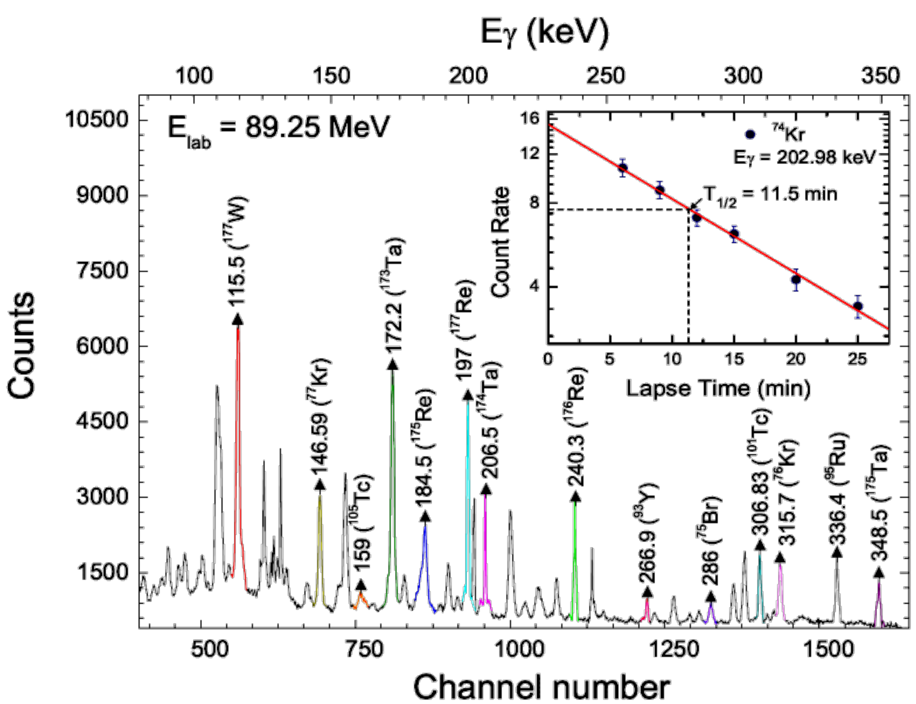

26 fission-like residues (32 ≤ Z ≤ 49) were identified in the present work

Decay data for fission-like residues

Serial No.	E_γ (keV)	I_γ (%)	Nuclide	Half-life ($T_{1/2}$)
1	728, 634.8	35.6, 91.2	$^{74}Br^m$	46 min
2	202.98	18	^{74}Kr	11.50 min
3	286	88	^{75}Br	96.7 min
4	264	11.4	^{75}Ge	82.78 min
5	154.6	21.1	^{75}Kr	4.29 min
6	315.7	39	^{76}Kr	14.8 h
7	146.59	37	^{77}Kr	74.4 min
8	613.8	54	^{78}As	90.7 min
9	668.1	23.4	^{79}Rb	22.9 min
10	443.3	17	^{81}Sr	22.3 min
11	881	98	^{84}Br	31.76 min
12	454	40	^{85}Zr	7.86 min
13	627.7	32.6	^{86}Y	14.74 h
14	201	96.4	^{87}Zr	1.68 h
15	947.7	10	^{89}Rb	15.15 min
16	266.9	7.4	^{93}Y	10.18 h
17	367.2	75	^{94}Ru	51.8 min
18	336.4	69.9	^{95}Ru	1.64 h
19	657.8	98.2	^{97}Nb	72.1 min
20	657.8	98.2	$^{98}Nb^m$	51.3 min
21	306.83	89	^{101}Tc	14.02 min
22	630.2	16.1	$^{102}Tc^m$	4.35 min
23	358	89	^{104}Tc	18.3 min
24	941.6	25	^{104}Ag	69.2 min
25	159	10.2	^{105}Tc	7.6 min
26	787.3	93.4	^{105}In	5.07 min

Post fission observable : Mass yields of fission fragments

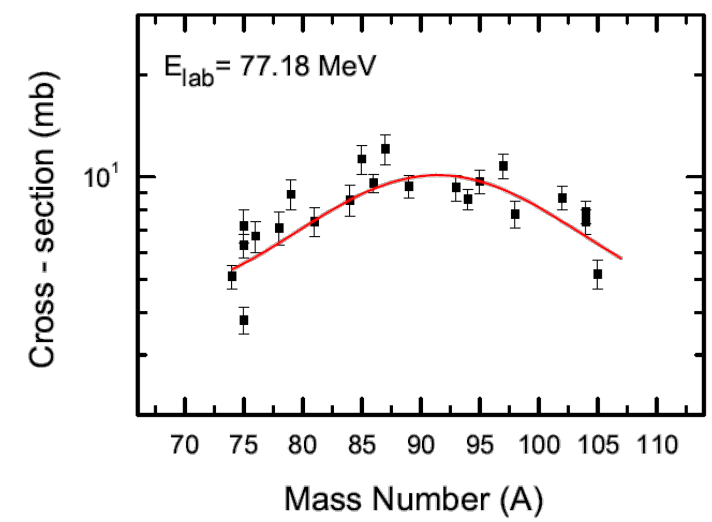

- **Mass yields of fission fragments at E_{lab} ≈ 77.18 MeV**
- **Symmetric mass yields → production via compound nuclear process.**
- **Similar results are obtained at 89.25 and 83.22 MeV**

Observations

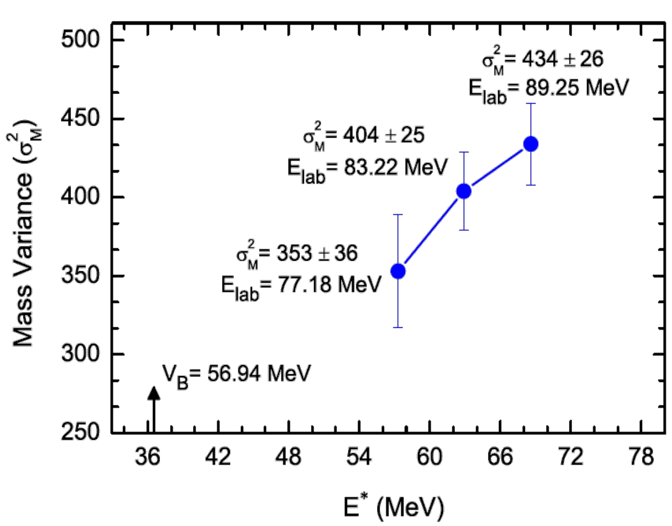

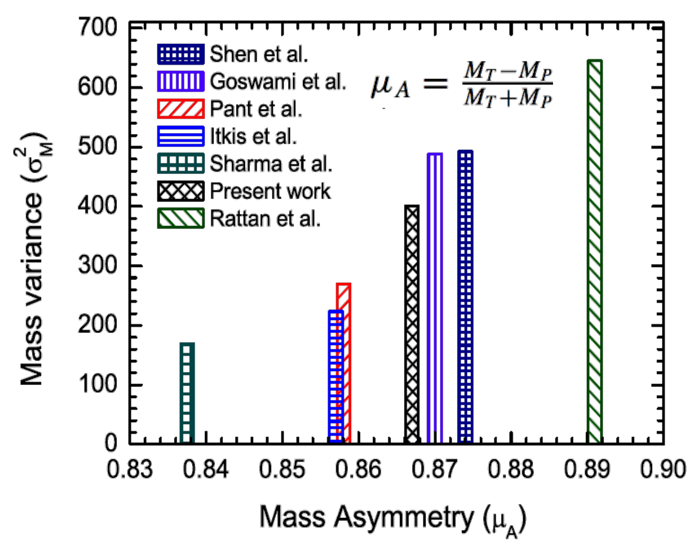

- **σ_M^2 decreases with the decrease in E* for deformed Tm target**
- **Similar trend reported by Ghosh et al., (Phys. Lett. B 627, 26 (2005)) for deformed Th target.**
- **σ_M^2 increases with the increase in mass asymmetry**

FISSION-LIKE EVENTS IN $^{12}C + ^{169}Tm$ REACTION AT LOW E*

Isotopic and Isobaric yield distribution of ^{74,75,76,77}Kr and ^{101,102m,104,105}Tc at E_{lab} = 83.22 and 89.25 MeV

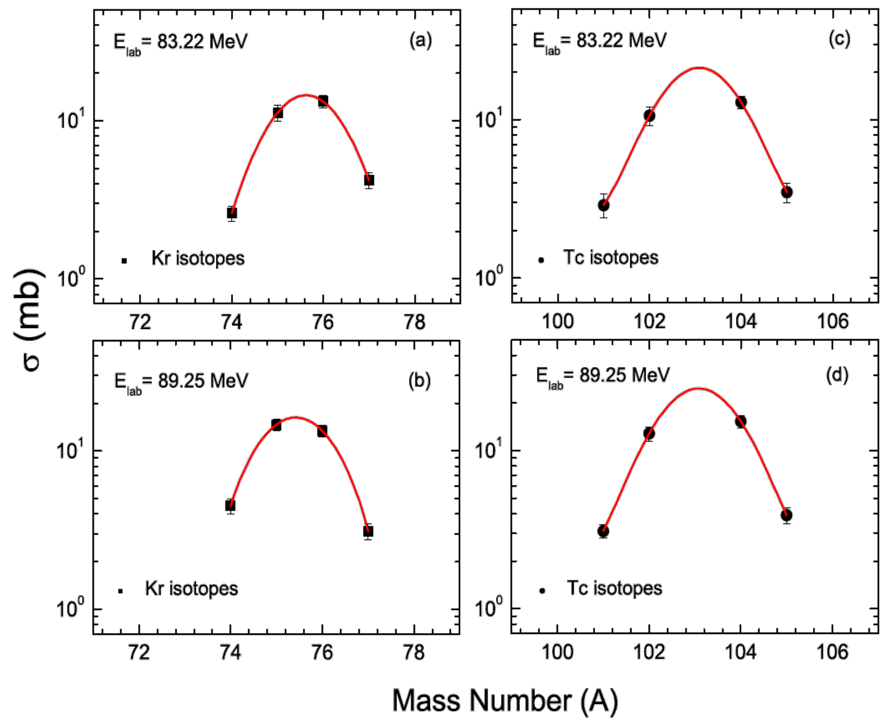

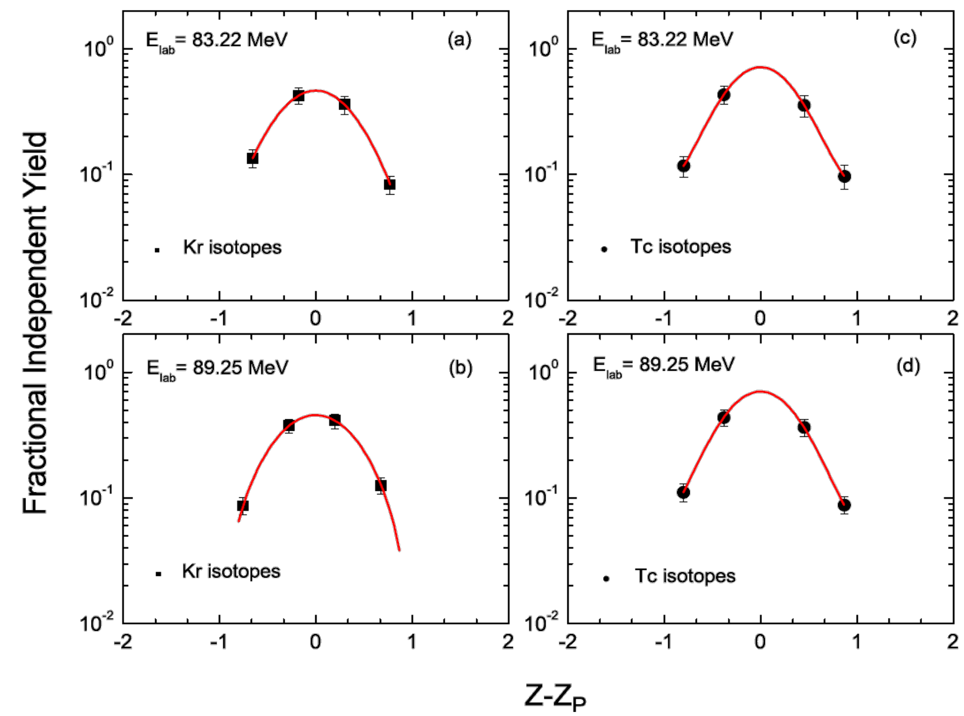

Variance of isotopic yield distribution for different systems

System	E^* (MeV)	Isotope	σ_A^2
$^{12}C + ^{169}Tm$	68.6	Kr	3.90 ± 0.20
$^{12}C + ^{169}Tm$	68.6	Tc	3.27 ± 0.18
$^{12}C + ^{169}Tm$	62.9	Kr	3.05 ± 0.18
$^{12}C + ^{169}Tm$	62.9	Tc	2.94 ± 0.28
$^{16}O + ^{181}Ta$	67.04	Y	3.05 ± 0.10
$^{16}O + ^{181}Ta$	67.04	In	4.16 ± 0.01
$^{16}O + ^{159}Tb$	57.1	Sr	3.31
$^{16}O + ^{159}Tb$	57.1	Y	4.41
$^{16}O + ^{169}Tm$	61.06	In	4.24
$^{16}O + ^{169}Tm$	61.06	Tc	4.62
$^{7}Li + ^{232}Th$	41.7	Sb	4.08
$^{7}Li + ^{232}Th$	41.7	I	3.96
$^{11}B + ^{232}Th$	55.7	Sb	4.0
$^{11}B + ^{232}Th$	55.7	I	5.43
$^{11}B + ^{232}Th$	55.7	Cs	3.72
$^{11}B + ^{238}U$	67.4	Rb	3.84 ± 0.16
$^{11}B + ^{238}U$	67.4	Cs	3.95 ± 0.14
$^{22}Ne + ^{238}U$	64.5	Rb	4.23 ± 0.40
$^{22}Ne + ^{238}U$	64.5	Cs	4.26 ± 0.90
$^{20}Ne + ^{208}Pb$	46.4	Sb	3.43 ± 1.02
$^{20}Ne + ^{208}Pb$	46.4	I	3.95 ± 0.87

EXPT. 02: REACTION DEPENDENT ENTRY STATE POPULATION: $^{12}C + ^{169}Tm$

REACTION DEPENDENT ENTRY STATE POPULATION: $^{12}C + ^{169}Tm$

Arshiya Sood et al., J. Phys. G: Nucl. Part. Phys. 48, 025105 (2021) ; Arshiya Sood et al., Acta Physica Polonica B 51, 775 (2020)

Motivation

- ICF → unexpected onset at slightly above barrier energies, i.e., 4-7 MeV/A, where CF is expected to be dominant.
- Paucity of studies that can furnish direct evidence for the bunch of angular momentum associated with various reaction channels → localization of ℓ window

The competition between the CF and ICF over ℓ window is not yet clearly understood!

- ICF → reported as a promising route to produce high spin states in final reaction products using HI beams even at low bombarding energies, although a perfect modelling is still apart!
- Role of target deformation and mass symmetry in ICF dynamics !

Experimental Details

Experiment : IUAC – GDA beamline

System : $^{12}C + ^{169}Tm$

Detector : Charged Particle Detector Array (CPDA)

- 14 CPDs divided into three angular regions :
  - 4 Forward (F) : 10°- 60°
  - 6 Sideways (S) : 60°- 120°
  - 4 Backward (B) : 120° - 170°

Gamma Detector Array (GDA)

- 12 Compton suppressed high resolution HPGe detectors at angles 45°, 99° and 153° with respect to the beam axis

Technique : Particle(p,α)- gamma coincidence

E_{lab} : ≈ 60-90 MeV (7 energies)

Schematics of detector arrangement

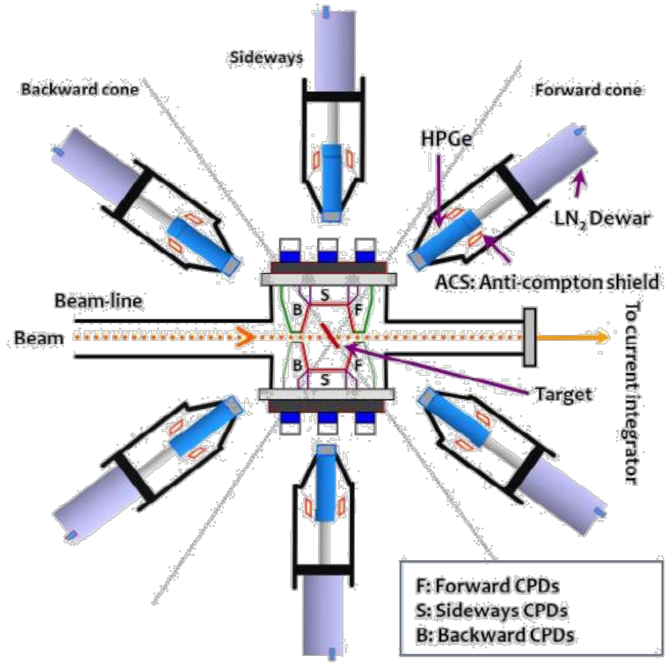

CPDA

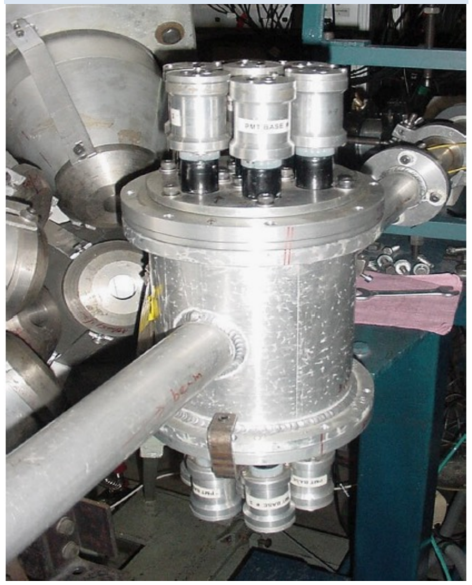

GDA

REACTION DEPENDENT ENTRY STATE POPULATION: $^{12}C + ^{169}Tm$

Data Reduction Methodology

- To identify pure xn channels → *singles spectra were recorded using two HPGe detectors at backward and forward angles*
- Coincidences were established between *particle (Z=1,2) and prompt gamma-rays*
- Measurements for *forward (F) and backward (B) CPDs* were used in the analysis
- Four gating conditions were projected on gamma spectra to generate particle and alpha gated spectra

Gating conditions

Forward cone } *forward-alpha-gated*, *forward-particle-gated*

Backward cone } *backward-alpha-gated*, *backward-particle-gated*

- Identification of reaction products → *characteristic prompt gamma-rays from singles and gated spectra*
- Intensities & area under photo peak were used to determine production yield

Evaporation α- profile : PACE4

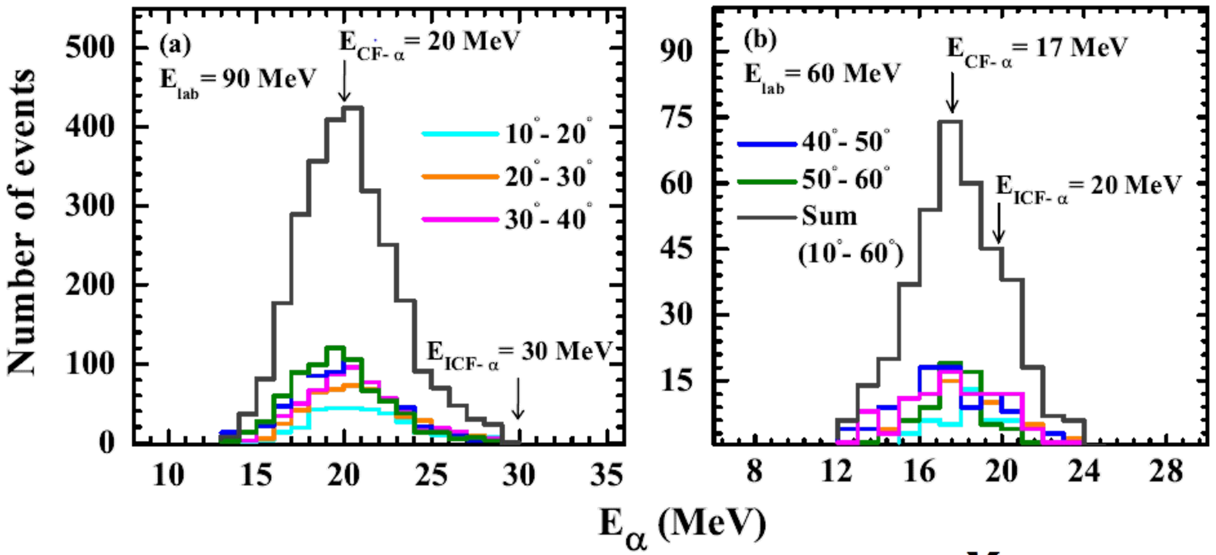

Energy of fast alphas $E_{ICF-\alpha} = E_P \times \frac{M_\alpha}{M_P}$

- Both *evaporation (slow)* and *direct (fast) alphas* can be detected in F –CPDs
- *Aluminum (Al) absorbers* of sufficient thickness were used to *stop slow alphas*
- Corrected F-α -gated → *(F-α-gated) – (B- α-gated)*

→ Production yields of ERs are plotted as a function of experimentally observed spin J_{obs} to obtain gamma-transition intensity patterns of different reaction products

$$Y = \frac{Y_\circ}{1 + exp(J_{obs} - J_\circ)/\Delta}$$

J_0 → mean input angular momentum (< ℓ >) (Barker et al., Phys. Rev. Lett. 45 (1980) 424)

REACTION DEPENDENT ENTRY STATE POPULATION: $^{12}C + ^{169}Tm$

Gamma transition intensity patterns: α3n, 5n and 2α2n channels

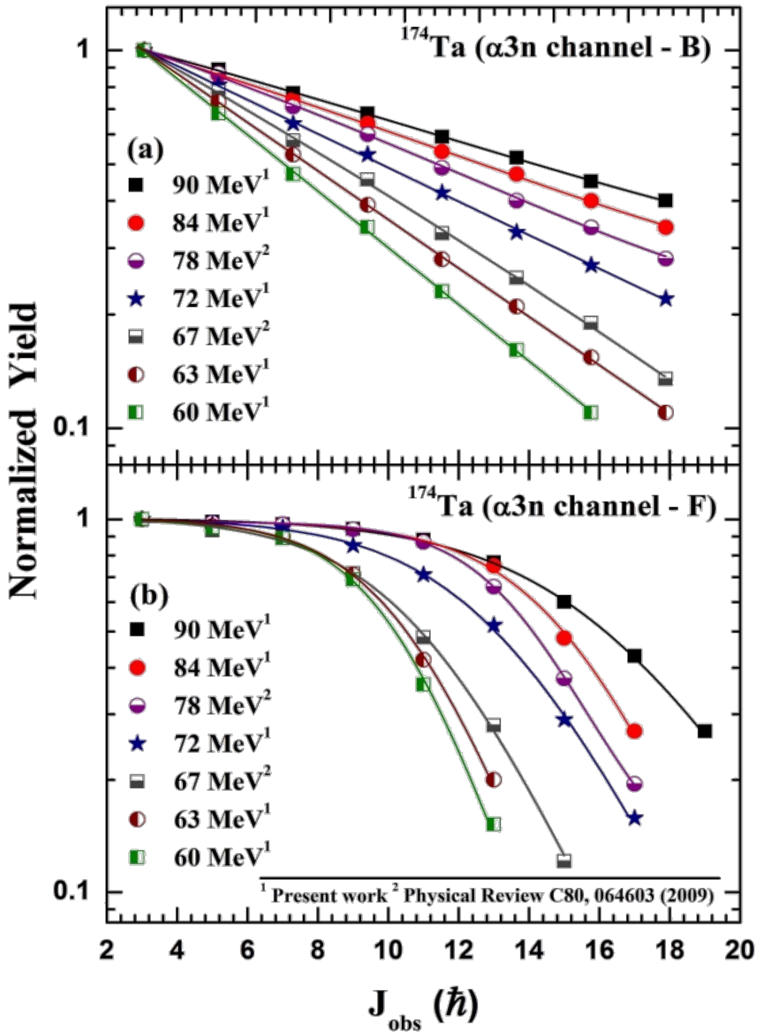

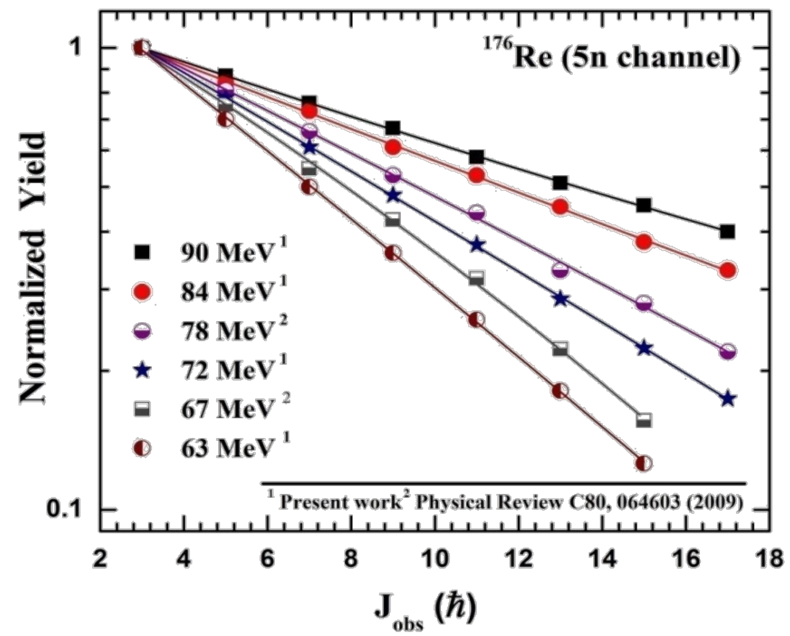

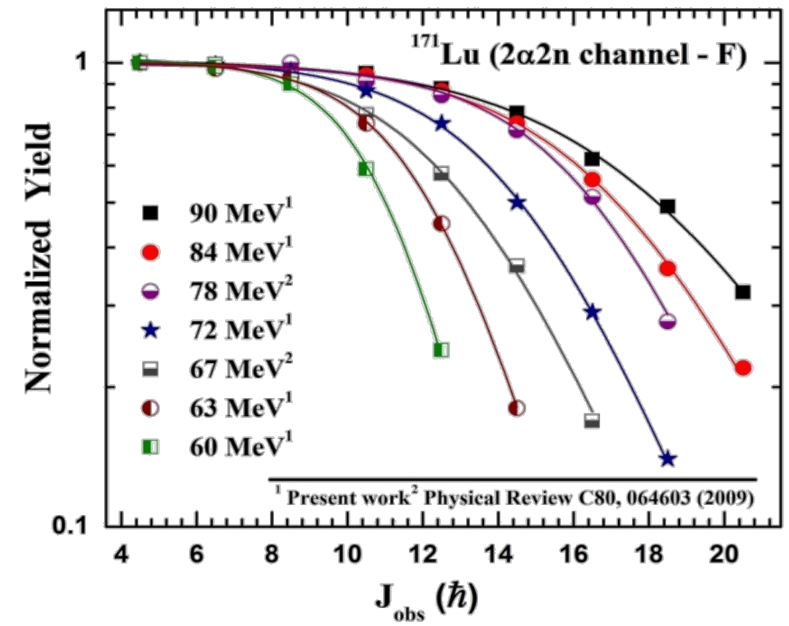

Feeding intensity profile for CF and ICF channels @ 90 and 84 MeV

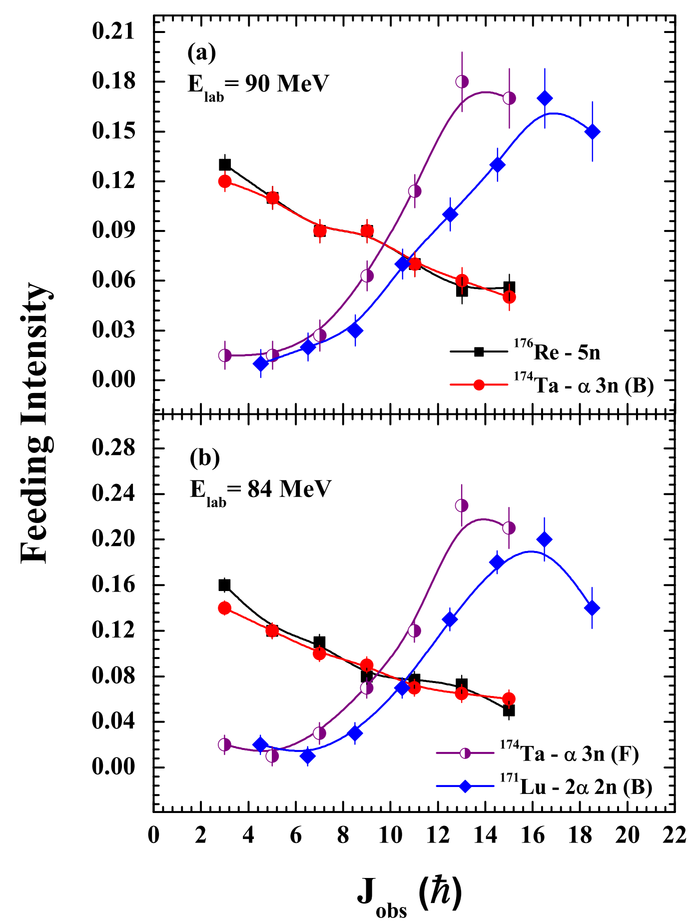

CF (backward- α- gated) : intensity increases towards band head →

population of broad spin range and/or strong feeding of low spin states towards band head.

ICF (forward- α- gated) : intensity increases down to some extent after which yields do not change towards the band head →

absence of feeding to low spin states and/or the population of low spin states is strongly hindered

$$\Delta N(J) = N_\gamma(J+2 \rightarrow J) - N_\gamma(J+4 \rightarrow J+2)$$

where, $\Delta N(J)$ and N_γ refer to the normalized yield difference and normalized yields for the gamma transitions given in the parenthesis, respectively.

CF: spans broad spin range

ICF : confined to narrow spin range on high spin side

REACTION DEPENDENT ENTRY STATE POPULATION: $^{12}C + ^{169}Tm$

Higher ℓ- values in α-emitting ICF channels

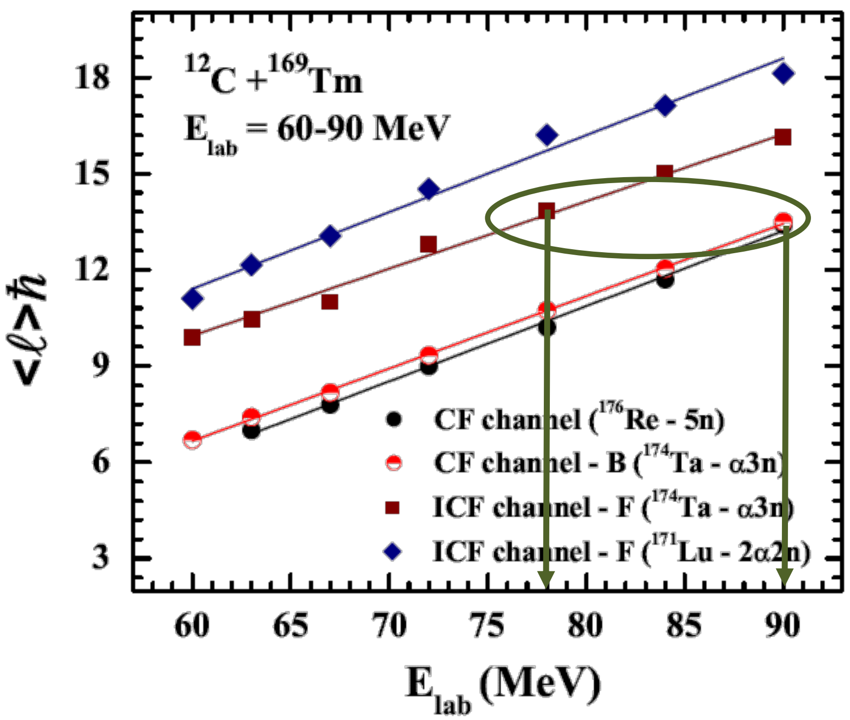

For same α-channel → ICF can populate high spin state at low projectile energy than CF

- ℓ values of ICF -2αxn and -αxn channels are 35-74% and 20-50% higher as compared to CF-xn channels, respectively

ICF reactions → possibly an advantageous tool to access **high spin states in the residual nucleus even at low projectile energies** which is not otherwise possible

Entrance channel dependence of ICF

Compilation of present data and data existing in literature

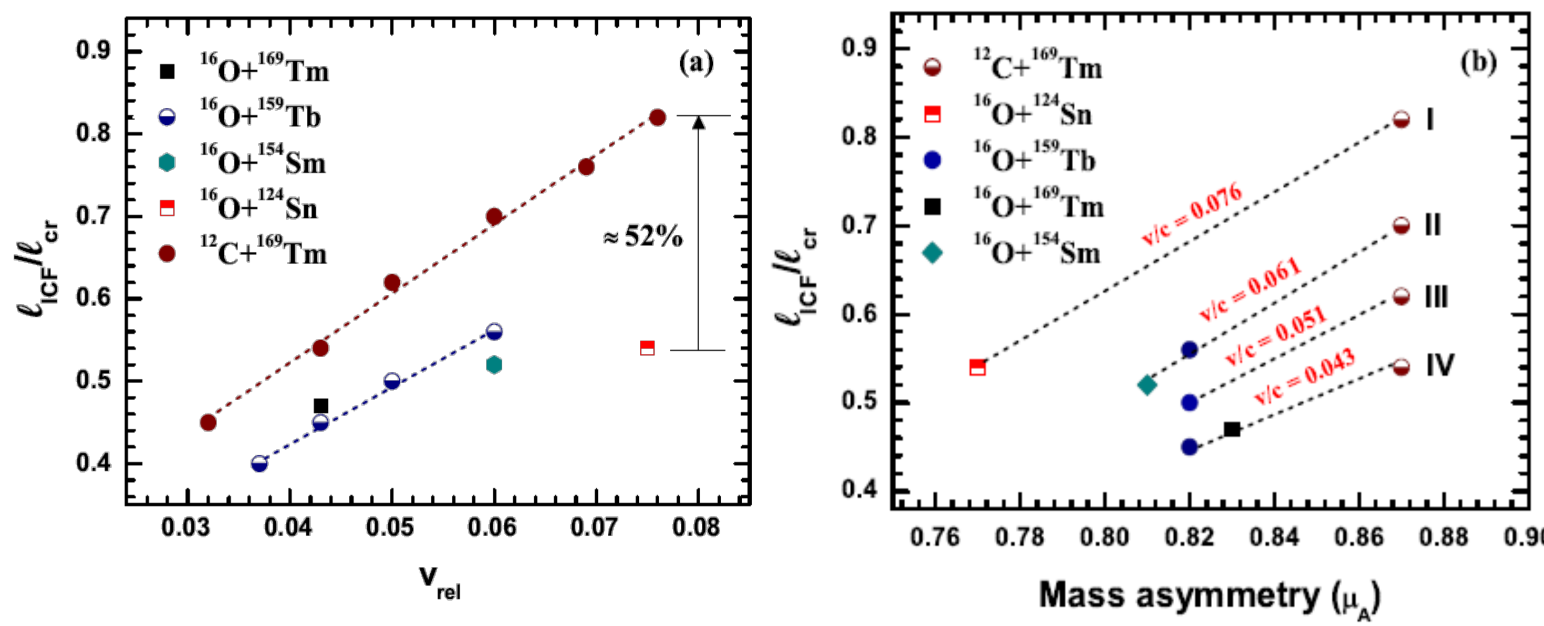

- Input angular momentum increases with the increase in relative velocity.
- Pronounced increase in input angular momentum for deformed target.
- For a constant v/c, value of input angular momentum is higher for more mass asymmetric system

Mass asymmetry and deformation play a significant role in ICF dynamics!!

EXPT. 03: QUASI-ELASTIC BACKSCATTERING IN ^{7}Li+ ^{116,118}Sn SYSTEMS

QUASI-ELASTIC BACKSCATTERING IN ^{7}Li+ ^{116,118}Sn SYSTEMS

Arshiya Sood et al., (Manuscript in preparation - collaboration with Prof. Lubian, Instituto de Física da UFF, Brazil)

Motivation

- Near barrier HI fusion is strongly influenced by the internal structure of the colliding nuclei and interconnectivity to different reactions resulting in Fusion Barrier Distribution
- Rowley et al. suggested a novel method to extract barrier distribution from fusion cross-sections as (Phys. Lett. B 254 (1991) 25)

$$D_{fus}(E) = \frac{d^2}{dE^2}\left[E\sigma_{fus}(E)\right]$$

- Disadvantage : involves second derivative → fusion cross-sections have to be measured very precisely
- Quasielastic (QEL) scattering - sum of all reaction processes other than fusion (elastic, inelastic, transfer, breakup...) → complementary to fusion (T+R=1 ⇒ dT/dE = - dR/dE)
- Timmers et al. suggested to obtain QEL barrier distribution as (Nucl. Phys. A 584 (1995) 190)

$$D_{qel}(E) = -\frac{d}{dE}\left[\frac{d\sigma_{qel}}{d\sigma_{Ruth}}(E)\right]$$

- Experimental advantages of D_{qel}
  - involves first derivative → can be extracted from data - less precision required
  - QEL excitation function → easy to measure than fusion at low energies → well suited for future experiments with low energy exotic beams.
- For tightly bound systems, fusion is dominant near the barrier → $D_{qel} \approx D_{fus}$ (qel = elastic+inelastic)
- For weakly bound systems, at near barrier energies fusion, breakup /transfer compete → shift in D_{qel}

Weakly bound nuclei

- Cluster/halo structure - ^{6}Li : α+d, ^{7}Li : α+t, ^{9}Be : α +α+n
- Low breakup threshold - 1.48 – 2.45 MeV → breakup is an important reaction channel

Experimental Details

Experiment :	IUAC – GPSC beamline
System :	^{7}Li + ^{116,118}Sn (≈ 380,430 μg/cm^{2})
Facility :	General Purpose Scattering Chamber (GPSC)
Detector :	Particle identification → HYbrid Telescope ARray (HYTAR) – 13 detectors @ 36°-173° • Each unit comprises of gas ionization chamber (ΔE) followed by a Si - detector (E_{res}) • 7mm thick collimators to define the solid angles Beam monitoring and nomalization → Monitor detectors @ ± 10°
E_{lab} :	14.88 – 28.92 MeV (corrected for energy loss) • 30% below- to above-barrier ($V_{B\,(lab)}$ ≈ 21.33 MeV) • Energy changed in steps of 2MeV below barrier and 3MeV above barrier

Detector set-up in GPSC

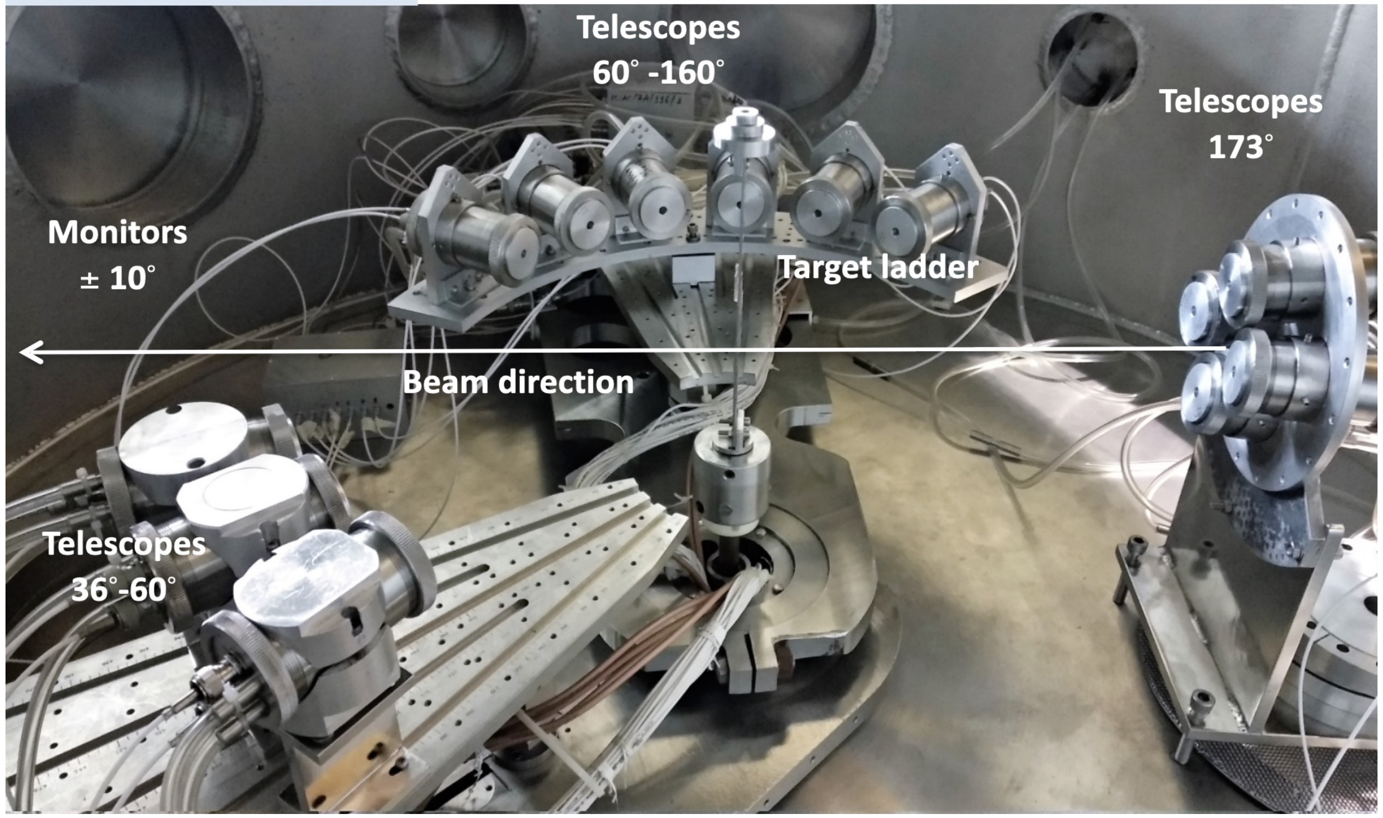

QUASI-ELASTIC BACKSCATTERING IN ^{7}Li+ ^{116,118}Sn SYSTEMS

Schematics of detector set-up used for QEL measurements

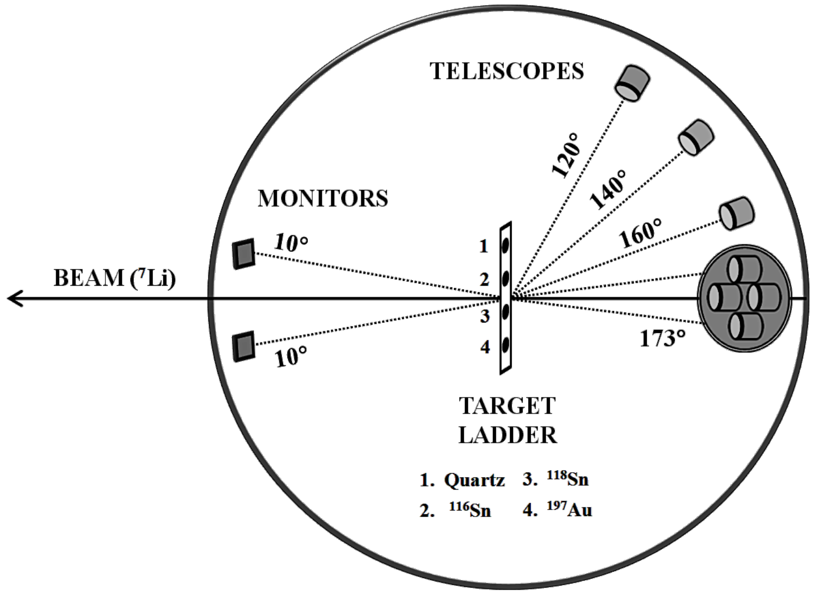

Advantage

- For measurements done at $\theta_{lab} < 180°$, the "effective" c.m. energies corresponding to each angle can be obtained using the relation

$$E_{eff} = \frac{2E_{c.m.}}{1+\mathrm{cosec}(\theta_{c.m.}/2)}$$

- measurements can be performed simultaneously at four different energies corresponding to 120°, 140°, 160°, 173° for a single beam energy

Such a setup improves the efficiency of the experiment, and allows to use small energy steps required for better barrier distributions.

Typical ΔE-E$_{res}$ spectra for ^{7}Li + ^{116,118} Sn reactions @ E$_{lab}$= 23 MeV and θ_{lab} =160^{0}, E$_{eff}$ = 21.48 MeV

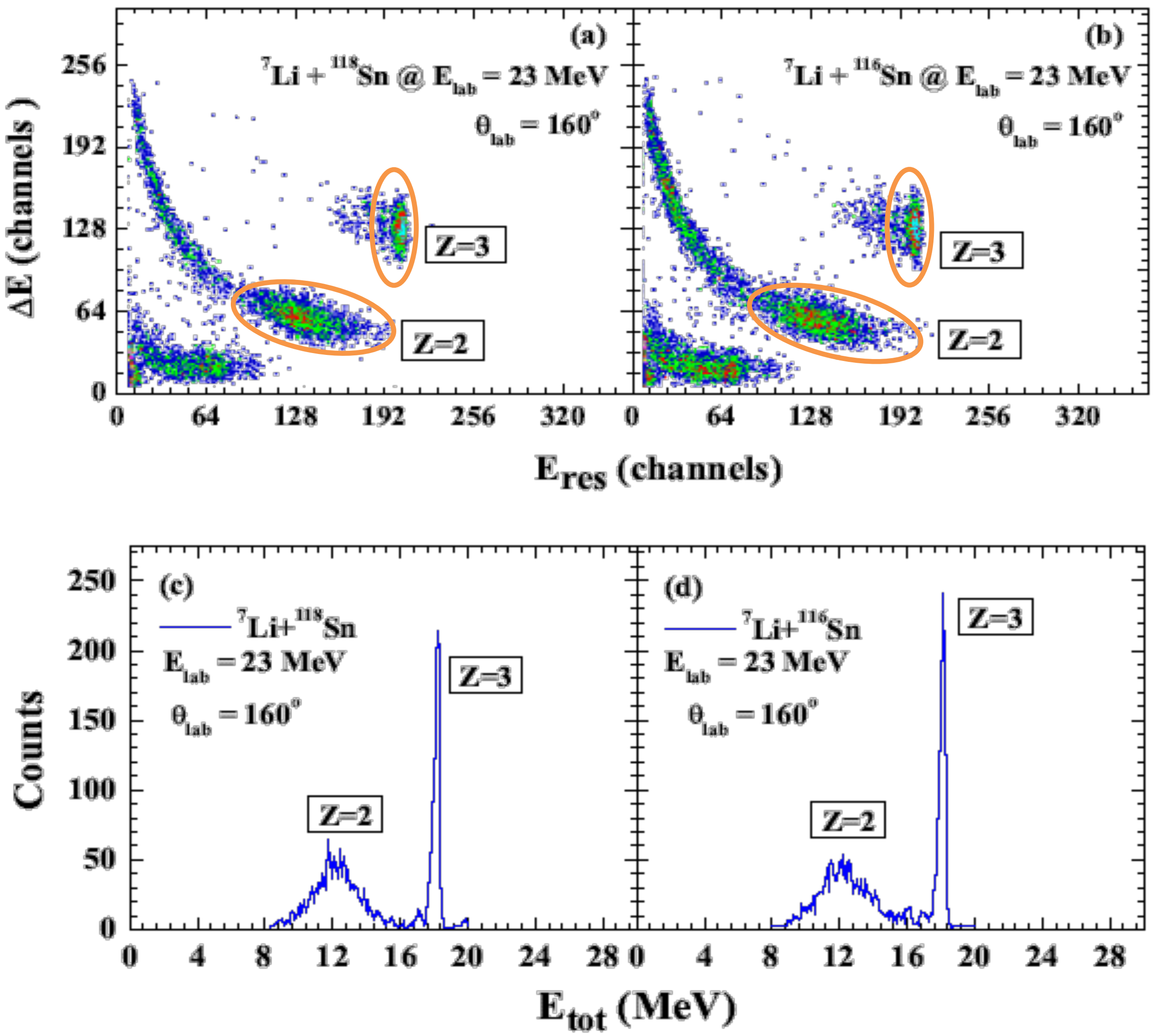

Projections of the lobed portions of Z=3 and Z=2 bands on total energy axis

Broad continuous peak – centroid at 12.2 MeV (4/7 * beam energy at θ_{lab} =160^{0})

QUASI-ELASTIC BACKSCATTERING IN ^{7}Li+ ^{116,118}Sn SYSTEMS

- ***The ratio QEL/Rutherford scattering is obtained by the relation***

$$\frac{d\sigma_{qel}}{d\sigma_{Ruth}}(E,\theta_{tel}) = \left[\frac{N_{tel}(E,\theta_{tel})}{N_{mon}(E,\theta_{mon})}\right] \times \left[\frac{\Delta\Omega_{mon}}{\Delta\Omega_{tel}}\right] \times \left[\frac{(d\sigma_{Ruth}/d\Omega)(E,\theta_{mon})}{(d\sigma_{Ruth}/d\Omega)(E,\theta_{tel})}\right]$$

where N_{tel} and N_{mon} are the number of events detected in the telescope and monitor detector at angle θ_{tel} and θ_{mon}, respectively, and $\Delta\Omega_{tel}$ and $\Delta\Omega_{mon}$ are the corresponding solid angles. $d\sigma_{Ruth}/d\Omega(E,\theta_{mon}(\theta_{tel}))$ is the calculated Rutherford cross-section at energy E and monitor angle θ_{mon} (telescope angle θ_{tel}). The

- ***The solid angle ratio was calculated from ^{7}Li+^{197}Au scattering at lowest incident energies using Rutherford formula***

$$\left[\frac{\Delta\Omega_{mon}}{\Delta\Omega_{tel}}\right] = \left[\frac{N_{mon}^{Au}(\theta_{mon})}{N_{tel}^{Au}(\theta_{tel})}\right]\left[\frac{(d\sigma_{Ruth}/d\Omega)_{Au}(\theta_{tel})}{(d\sigma_{Ruth}/d\Omega)_{Au}(\theta_{mon})}\right]$$

- ***Barrier distributions are obtained from QEL scattering cross-sections using the point-difference formula***

$$D_{qel}(E') = \frac{f(E_2) - f(E_1)}{E_2 - E_1}$$

where, $-f(E) = d\sigma_{qel}/d\sigma_{Ruth}$ for two energy points E_1 and E_2 and $E' = \frac{1}{2}(E_2 + E_1)$

QUASI-ELASTIC BACKSCATTERING IN $^{7}Li+ ^{116,118}Sn$ SYSTEMS

QEL cross-section ratio relative to Rutherford measured at different angles and their respective E_{eff} for $^{7}Li + ^{118}Sn$

			$^{7}Li+^{116}Sn$		$^{7}Li+^{118}Sn$	
E_{lab} (MeV)	θ_{lab}	E_{eff} (MeV)	$d\sigma_{qel}/d\sigma_{Ruth}$ (el.+inel.)	$d\sigma_{qel}/d\sigma_{Ruth}$ (el.+inel.+α)	$d\sigma_{qel}/d\sigma_{Ruth}$ (el.+inel.)	$d\sigma_{qel}/d\sigma_{Ruth}$ (el.+inel.+α)
14.88	120°	13.14	0.999 ± 0.020	0.999 ± 0.020	1.012 ± 0.021	1.012 ± 0.021
	140°	13.66	0.983 ± 0.023	0.983 ± 0.023	0.988 ± 0.023	0.988 ± 0.023
	160°	13.95	0.981 ± 0.026	0.981 ± 0.026	0.987 ± 0.026	0.987 ± 0.026
	173°	14.04	0.992 ± 0.030	0.992 ± 0.030	1.006 ± 0.031	1.006 ± 0.031
16.89	120°	14.91	0.998 ± 0.020	0.998 ± 0.020	1.010 ± 0.021	1.010 ± 0.021
	140°	15.50	0.989 ± 0.023	0.989 ± 0.023	0.969 ± 0.023	0.969 ± 0.023
	160°	15.83	0.971 ± 0.026	0.971 ± 0.026	0.958 ± 0.025	0.958 ± 0.025
	173°	15.93	0.949 ± 0.029	0.949 ± 0.029	0.947 ± 0.029	0.947 ± 0.029
18.90	120°	16.69	0.939 ± 0.019	0.939 ± 0.019	0.961 ± 0.021	0.961 ± 0.021
	140°	17.35	0.867 ± 0.020	0.867 ± 0.020	0.872 ± 0.023	0.872 ± 0.023
	160°	17.72	0.810 ± 0.021	0.810 ± 0.021	0.803 ± 0.024	0.803 ± 0.024
	173°	17.83	0.786 ± 0.024	0.786 ± 0.024	0.761 ± 0.027	0.761 ± 0.027
20.90	120°	18.46	0.653 ± 0.013	0.769 ± 0.015	0.674 ± 0.013	0.792 ± 0.015
	140°	19.18	0.506 ± 0.012	0.660 ± 0.015	0.508 ± 0.012	0.668 ± 0.015
	160°	19.60	0.403 ± 0.011	0.587 ± 0.015	0.412 ± 0.011	0.592 ± 0.015
	173°	19.71	0.451 ± 0.016	0.632 ± 0.022	0.384 ± 0.014	0.567 ± 0.019
22.91	120°	20.23	0.303 ± 0.006	0.496 ± 0.010	0.285 ± 0.007	0.465 ± 0.010
	140°	21.03	0.185 ± 0.005	0.401 ± 0.010	0.179 ± 0.005	0.378 ± 0.009
	160°	21.48	0.143 ± 0.004	0.356 ± 0.010	0.131 ± 0.004	0.332 ± 0.009
	173°	21.61	0.139 ± 0.006	0.358 ± 0.014	0.147 ± 0.008	0.344 ± 0.014
25.91	120°	22.88	0.066 ± 0.002	0.250 ± 0.007	0.061 ± 0.002	0.233 ± 0.005
	140°	23.78	0.037 ± 0.002	0.214 ± 0.009	0.029 ± 0.001	0.206 ± 0.005
	160°	24.29	0.021 ± 0.001	0.183 ± 0.011	0.019 ± 0.001	0.177 ± 0.005
	173°	24.44	0.028 ± 0.002	0.180 ± 0.011	0.022 ± 0.002	0.171 ± 0.006
28.92	120°	25.54	0.014 ± 0.001	0.158 ± 0.009	0.012 ± 0.001	0.144 ± 0.004
	140°	26.54	0.007 ± 0.001	0.142 ± 0.014	0.006 ± 0.001	0.119 ± 0.004
	160°	27.11	0.003 ± 0.001	0.131 ± 0.022	0.003 ± 0.001	0.113 ± 0.004
	173°	27.28	0.005 ± 0.001	0.133 ± 0.020	0.004 ± 0.001	0.109 ± 0.004

QUASI-ELASTIC BACKSCATTERING IN $^{7}Li + ^{116,118}Sn$ SYSTEMS

QEL excitation function and barrier distribution - elastic+inealstic :
Comparison of ^{116}Sn and ^{118}Sn isotopes

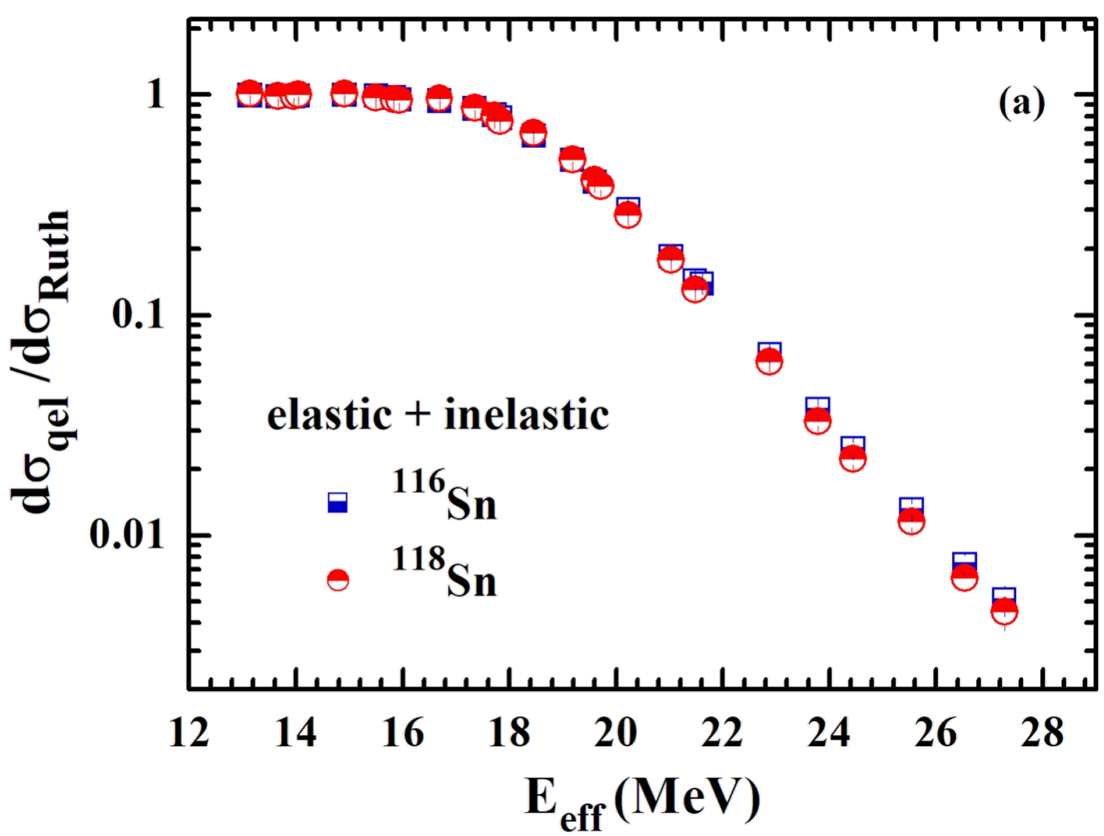

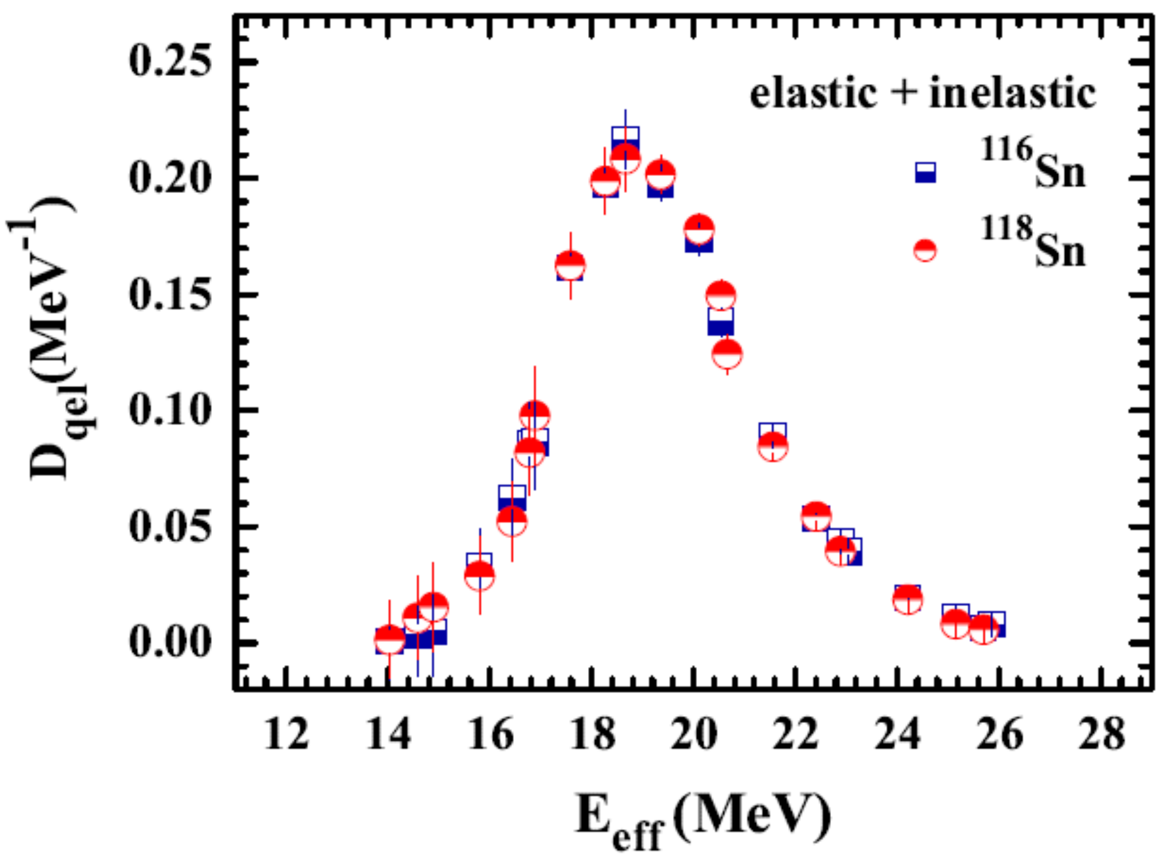

- *Cross sections for both the systems overlap down to lowest energies*
- *Barrier distributions peak at 19.2 MeV having the same shape and width.*

No isotopic dependence of quasi-elastic excitation function has been observed

QUASI-ELASTIC BACKSCATTERING IN ^{7}Li+ ^{116,118}Sn SYSTEMS

QEL excitation function and barrier distribution - elastic+inealstic : Comparison of experimental data with CC calculations using CCFULL (SC)

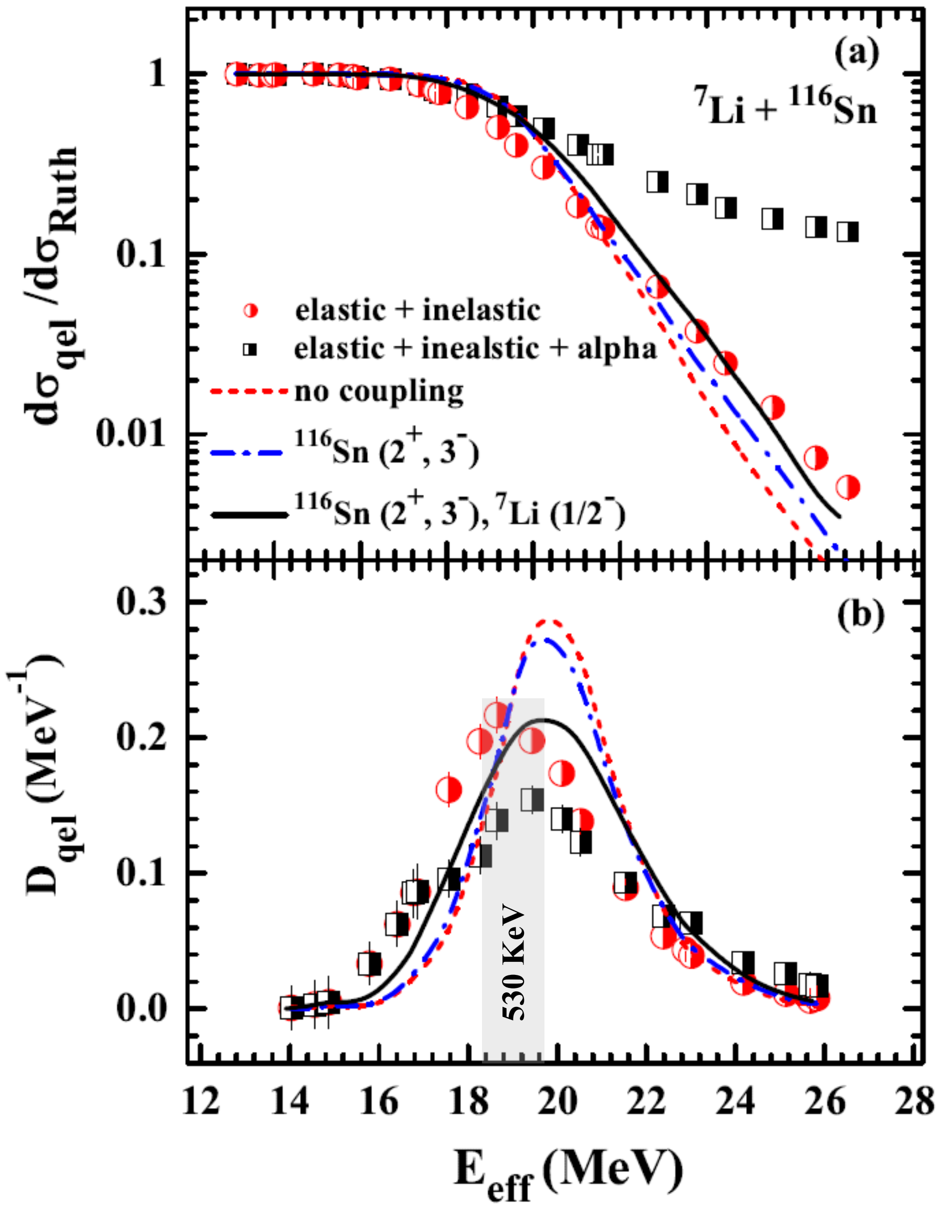

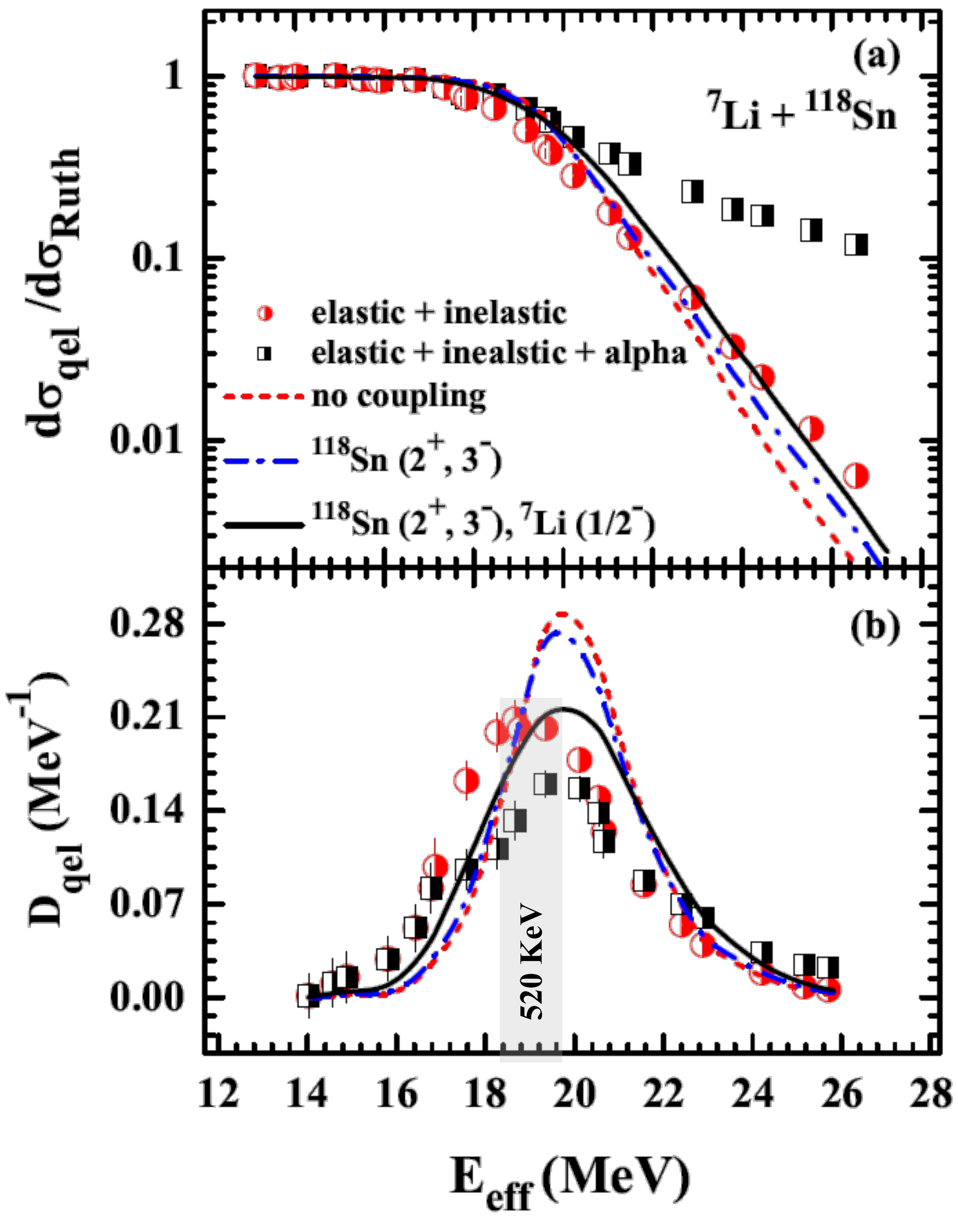

Peak position of theoretical barrier distribution (including coupling to $1/2^{-}$ state of ^{7}Li) is similar to experimental barrier distribution extracted from QEL excitation functions including elastic+inelastic+alpha - signature of effect of breakup and breakup like processes on fusion .

^{116,118}Sn – SELF-SUPPORTING TARGET FABRICATION

Arshiya Sood et al., Vacuum 172, 190107 (2020)

^{116,118} Sn targets were prepared in the Target laboratory at IUAC using High Vacuum deposition

High vacuum thin film deposition unit

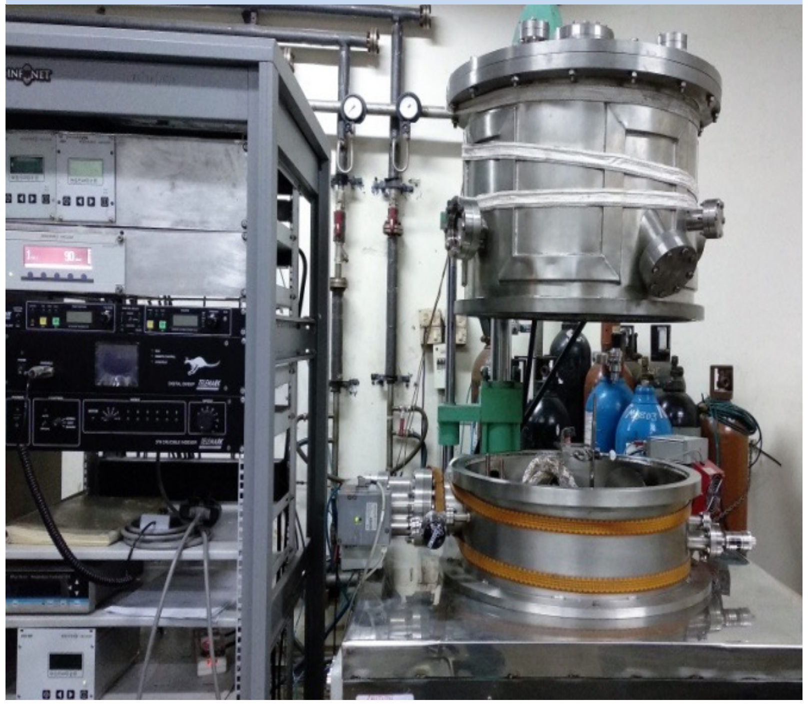

Top view of deposition set-up

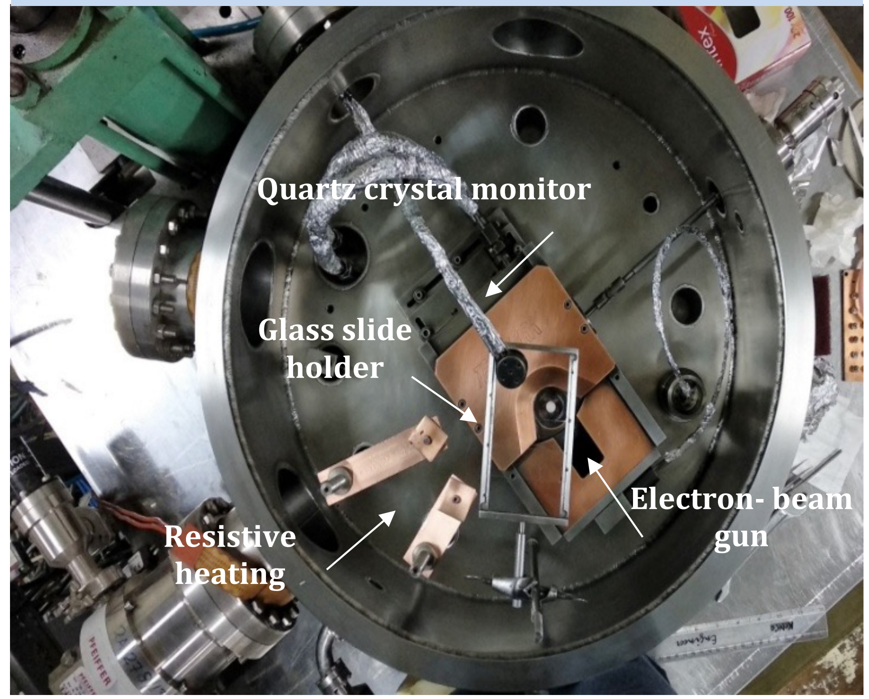

(a) Ta boat (b) Sn flakes (c) KCl pellet (d) Glass slide after deposition (e) scoring & floating of films

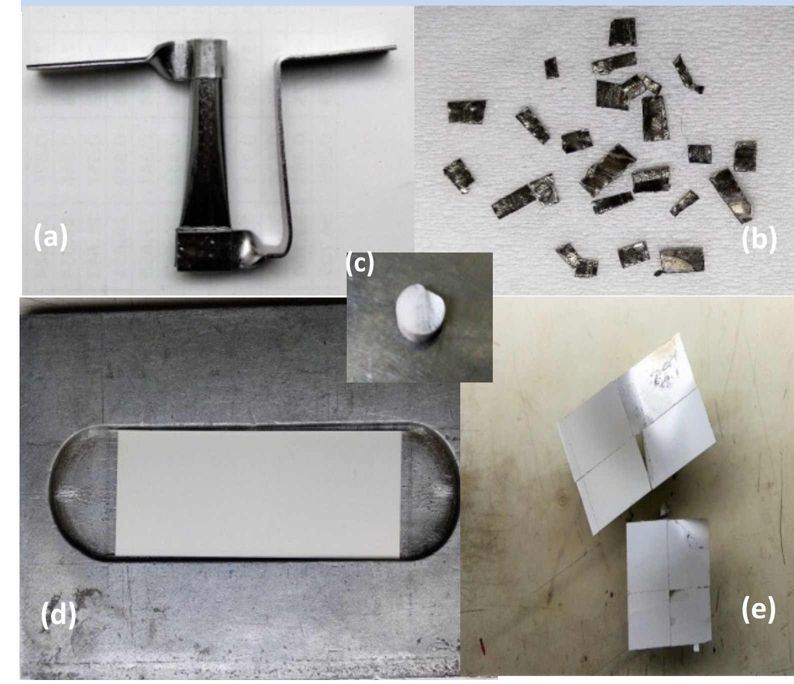

Films lifted on stainless steel frame after floating

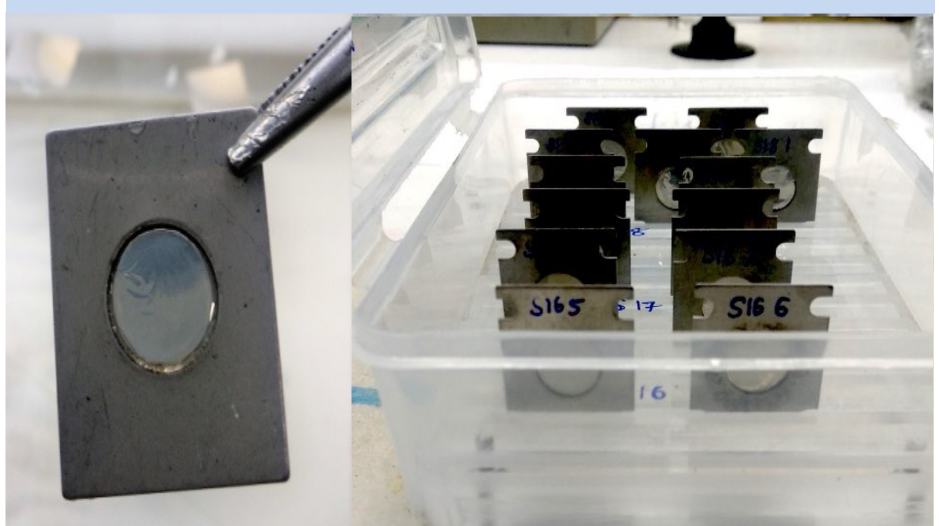

Comparison of present work on Sn targets with literature

Target	Target description	Fabrication method	Thickness (mg/cm^2)
^{116}Sn	Self-supporting	UHV evaporation	0.25-0.6
^{118}Sn	Self-supporting	UHV evaporation	0.25-0.6
^{112}Sn	Self-supporting	Cold Rolling	1
^{112}Sn	Self-supporting	Cold Rolling	8.4
^{116}Sn	Carbon (C) backed	HV evaporation	0.15
^{124}Sn	Aluminum (Al) backed	HV evaporation	0.2-0.35
^{112}Sn	Lead (Pb) backed	Cold Rolling	2.44, 10.26

116,118Sn – SELF-SUPPORTING TARGET FABRICATION

Characterization of ^{116,118} Sn targets – thickness , purity and stability

RBS spectra of ^{118}Sn with SIMNRA simulation

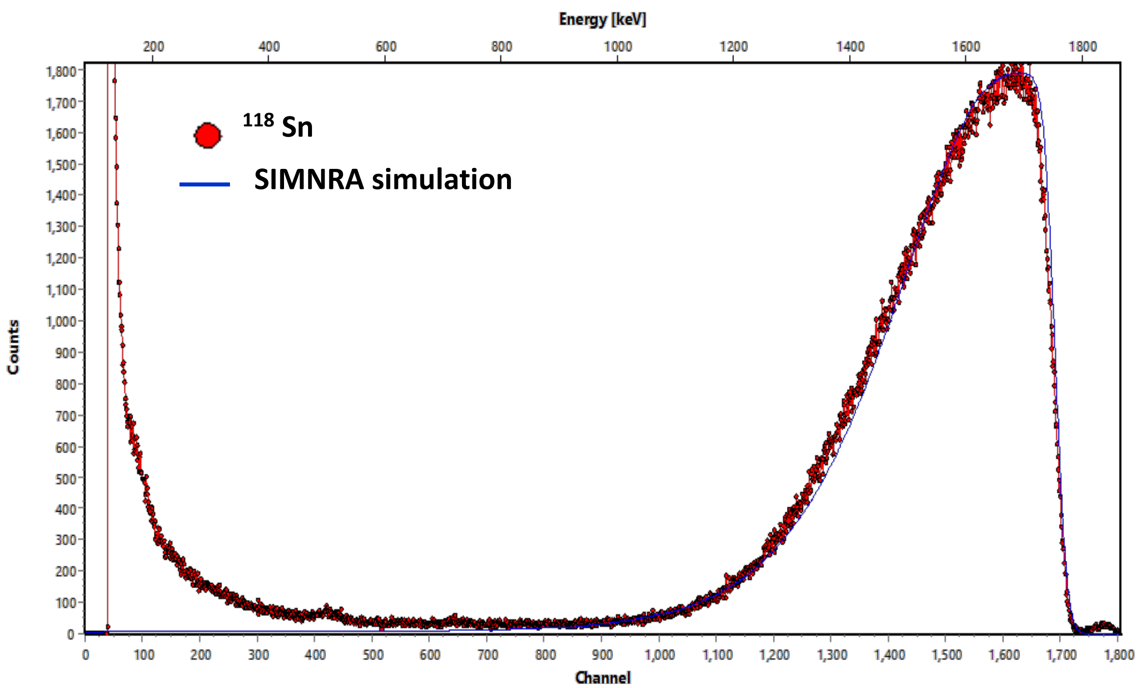

Alpha transmission spectra of ^{118}Sn

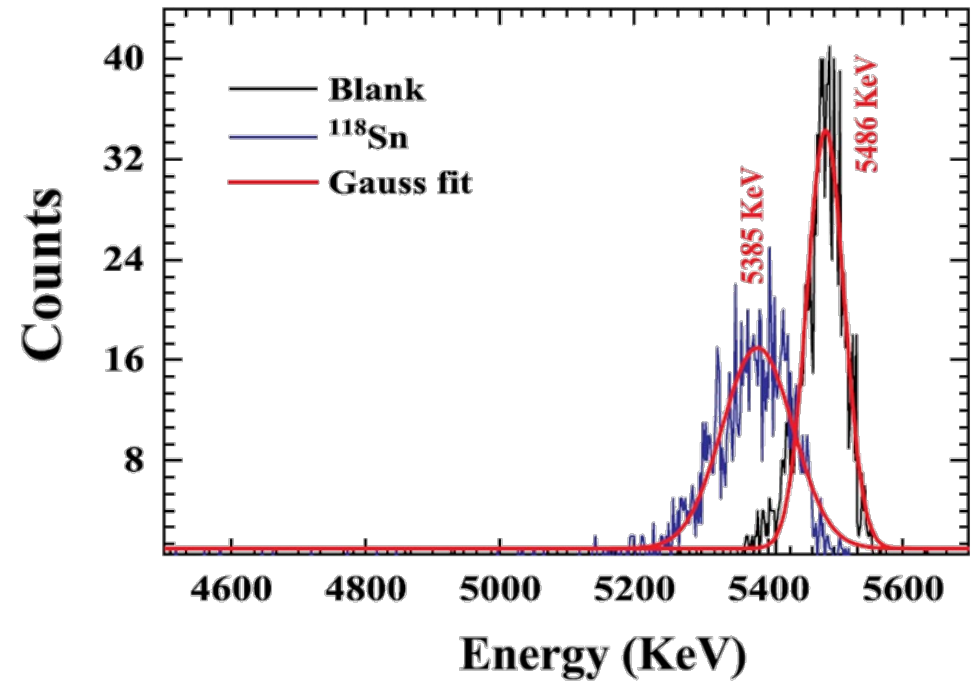

EDS spectra of ^{118}Sn (pristine and irradiated samples)

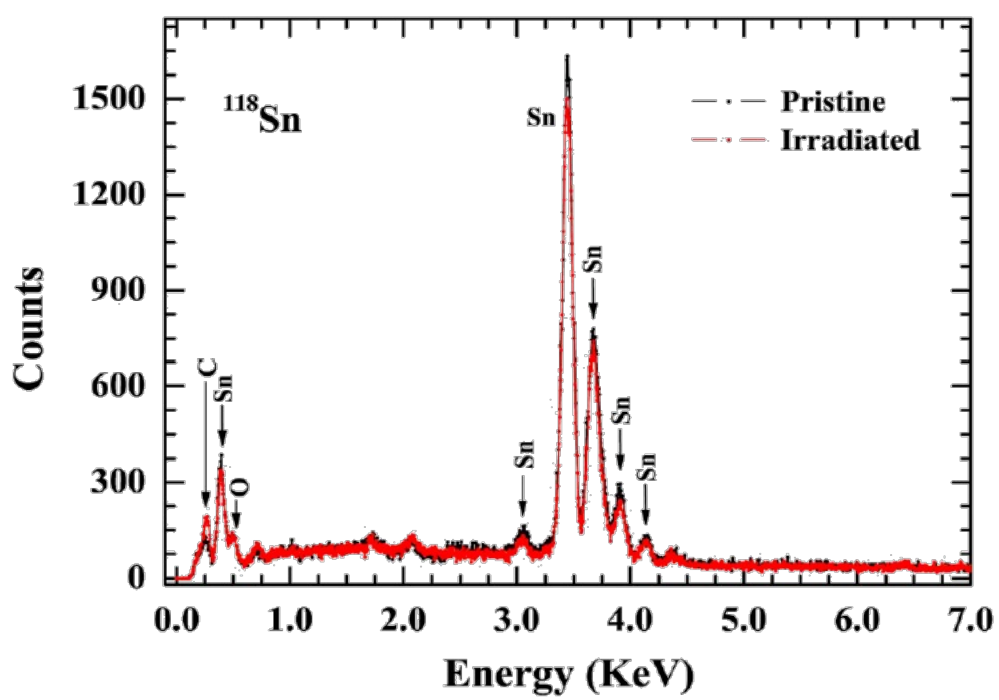

FTIR spectra of ^{118}Sn (pristine and irradiated samples)

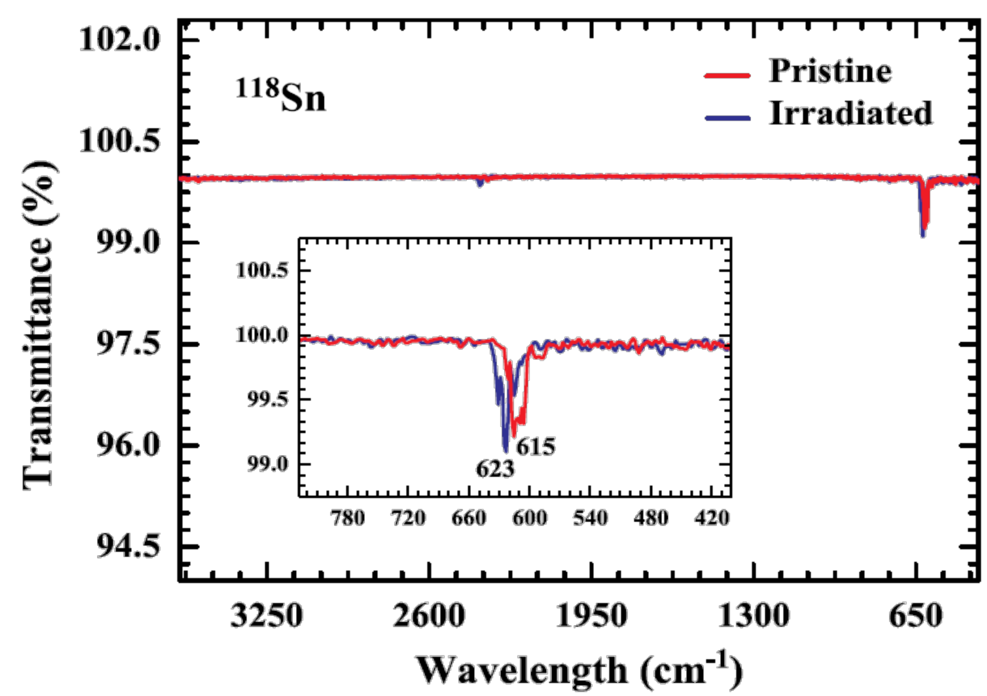

Results: Thickness of the fabricated targets varied from 0.25 - 0.6 mg/cm^2 . No residual gas (C, O or N) contamination was present.

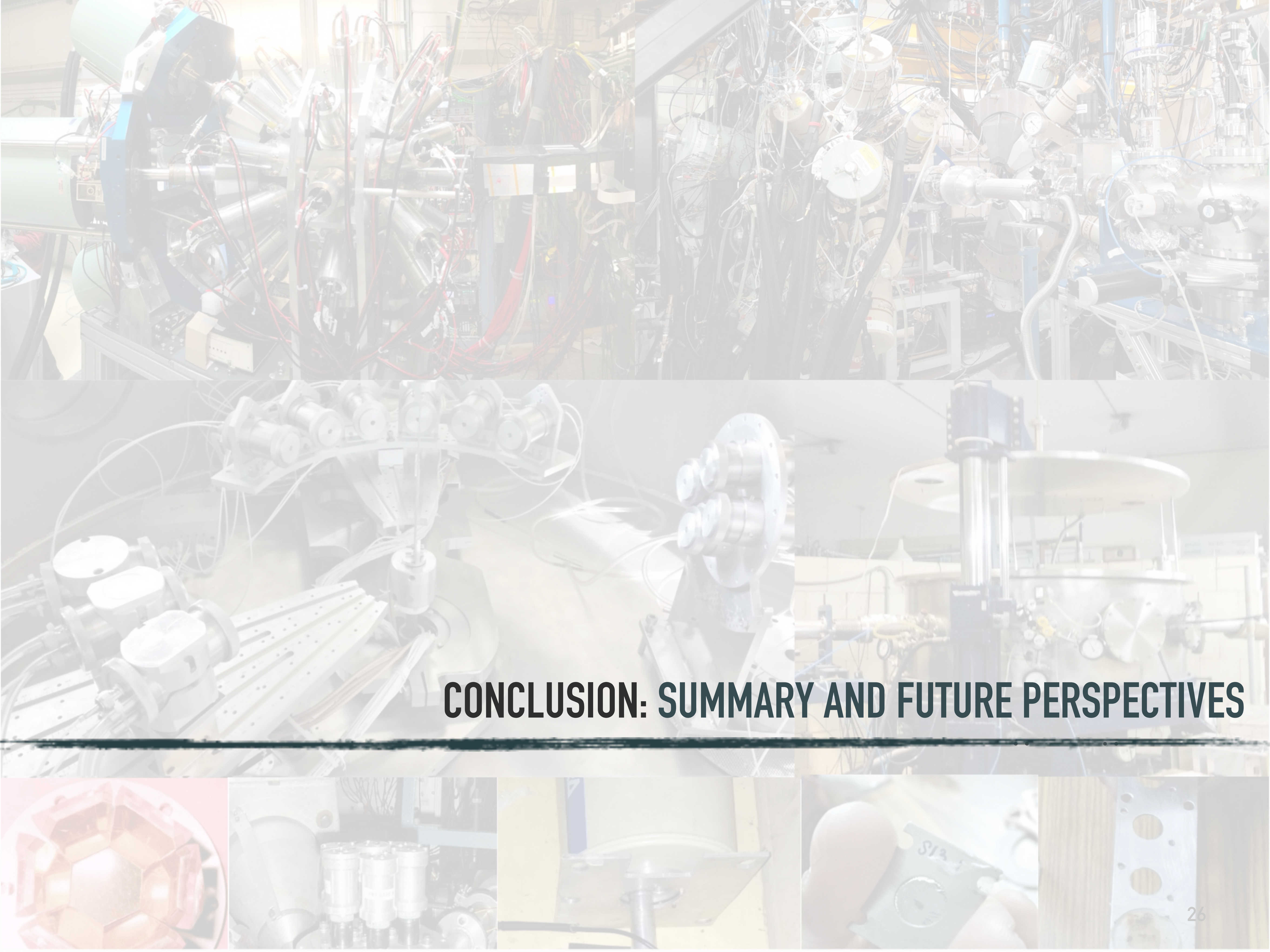

CONCLUSION: SUMMARY AND FUTURE PERSPECTIVES

SUMMARY AND FUTURE PERSPECTIVES

- ***Fission-like events***
  - *Production cross-sections of 26 fission-like residues ($32 \leq Z \leq 49$) were measured in $^{12}C+^{169}Tm$ system at E_{lab} = 89.25, 83.22, and 77.81 MeV.*
  - *Fission is found to be one of the modes of de-excitation at low excitation energies where LNPs and/or γ-rays are expected to be the sole contributors.*
  - *Mass yields were found to be nearly symmetric hinting at the absence of any non-compound nuclear process and is observed to be influenced by entrance channel parameters.*
  - *Isotopic and isobaric charge distributions were studied. Charge distribution parameters agree reasonably well with the experimental values reported in the literature.*
  - *More sophisticated experiments and analysis can be performed with different target (spherical and deformed) and projectile systems in the medium-mass region and at low excitation energies.*

- ***Gamma transition intensity patterns***
  - *Gamma transition intensity patterns of reaction products populated via xn, αxn and 2αxn - channels populated in CF and ICF in $^{12}C+^{169}Tm$ system at E_{lab} 5-7.5 MeV/A have been measured.*
  - *Gamma transition intensity patterns of CF and ICF products are found to be different corroborating the involvement of entirely different reaction dynamics in their production.*
  - *The analysis of ℓ values involved in the CF and ICF reactions suggests that ICF can populate high spin states at low projectile energies which are not otherwise possible to achieve.*
  - *Entrance channel mass-asymmetry and target deformation are observed to affect the ICF dynamics*
  - *Study of different projectile (α or non-α cluster) and target (deformed or spherical) combinations and comparison with present results would be very interesting and will further our understanding of ICF dynamics*

- ***Quasi-elasctic backscattering***
  - *QEL excitation functions were measured at θ_{lab} = 120°, 140° , 160° for the $^{7}Li+ ^{116,118}Sn$ systems at 30 % below- to above- barrier energies. The corresponding barrier distributions were derived from first derivative of experimental data.*
  - *Barrier distribution obtained from QEL excitation functions for elastic+inelastic+alpha channels are observed to shift towards higher energy side as compared to elastic+inelastic channels.*
  - *The discrepancy in the theoretical predictions and experimental results suggests that breakup and breakup like processes strongly influence fusion.*
  - *The CDCC calculations involving coupling to other important reaction channels like breakup and neutron transfer are essential for further understanding of the reaction dynamics and are being performed in collaboration with Prof. Lubian, Instituto de Física da UFF, Brazil.*

RESEARCH PUBLICATIONS

International peer-reviewed journals

1. **Fission-like events in the $^{12}C + ^{169}Tm$ system at low excitation energies.**
   Arshiya Sood et al.

   Physical Review C 96, 014620 (2017)
2. **Entrance Channel effects on fission fragment mass distribution in $^{12}C + ^{169}Tm$ system.**
   Arshiya Sood et al.

   Acta Physica Polonica B 50, 291 (2019)
3. **Self-supporting tin targets fabricated by ultra-high vacuum evaporation for heavy-ion induced reactions.**
   Arshiya Sood et al.
   Vacuum 172, 190107 (2020)

4. **Evidence of narrow range high spin population in incomplete fusion.**
   Arshiya Sood et al.

   Acta Physica Polonica B 51, 775 (2020)
5. **Disentangling complete and incomplete fusion events in $^{12}C + ^{169}Tm$ reaction by spin-distribution measurements.**
   Arshiya Sood et al.
   Journal of Physics G: Nuclear and Particle Physics 48, 025105 (2021)

6. **Quasi-elastic backscattering in $^{7}Li + ^{116,118}Sn$ systems.**
   Arshiya Sood et al.
   (Manuscript in preparation in collaboration with Instituto de Física da UFF, Rio de Janeiro, Brazil)

7. **Insights into the low-energy incomplete fusion**
   Rudra N. Sahoo, Malika Kaushik, **Arshiya Sood** et al.
   Nuclear Physics A 983, 145 (2019)

8. **Sub-barrier fusion in the $^{37}Cl + ^{130}Te$ system.**
   Rudra N. Sahoo, Malika Kaushik, **Arshiya Sood** et al.
   Physical Review C 99, 024607 (2019)

9. **Fabrication of thin ^{130}Te target foils for sub-barrier fusion studies.**
   Rudra N. Sahoo, G N Jyothi, **Arshiya Sood** et al.
   Nuclear Instruments and Methods in Physics Research Section A : Accelerators Spectrometers Detectors and Associated Equipment 935, 103 (2019)

10. **Entrance channel effect on incomplete fusion.**
    Rudra N. Sahoo, Malika Kaushik, **Arshiya Sood** et al.

    Acta Physica Polonica B 49, 585 (2018)

11. **Role of neutron transfer in sub-barrier fusion.**
    Rudra N. Sahoo, Malika Kaushik, **Arshiya Sood** et al.
    Physical Review C 102, 024615 (2020)

12. **Investigation of an intruder band in ^{45}Sc via Coulomb excitation.**
    M. Matejska-Minda with **Arshiya Sood et al.,**

    Acta Physica Polonica B 50, 411 (2019)

13. **Revised lifetime of the 11/2- state in ^{45}Sc via Coulomb excitation.**
    M. Matejska-Minda with **Arshiya Sood et al.,**

    Acta Physica Polonica B 51, 829 (2020)

14. **Effect of non-α-cluster projectile on incomplete-fusion dynamics: Experimental study of the $^{14}N + ^{180}Ta$ system.**
    M. Shariq Asnain with **Arshiya Sood et al.,**
    Physical Review C 104, 034616 (2021)

15. **Effect of Projectile structure on break-up fusion for $^{14}N + ^{175}Lu$ system at intermediate energies.**
    Ishfaq Majeed Bhat with **Arshiya Sood et al.,**
    Nuclear Physics A 1021, 122421 (2022)

16. **Role of precursor nuclei in heavy-ion induced reactions at low energies.**
    Ishfaq Majeed Bhat with **Arshiya Sood et al.,**
    Physical Review C 105, 054607 (2022)

17. **The DESPEC setup for GSI and FAIR.**
    A.K.Mistry with **Arshiya Sood et al.,**
    Nuclear Instruments and Methods in Physics Research Section A : Accelerators Spectrometers Detectors and Associated Equipment 1033, 166662 (2022)

Conference proceedings

1. **Observation of fission-like events in the $^{12}C + ^{169}Tm$ system at E* ≈ 69, 63, and 57 MeV.**
   Arshiya Sood et al.
   Proceedings of the DAE Symposium on Nuclear Physics 62, 544 (2017)

2. **Effect of target neutron skin thickness on incomplete fusion probability.**
   Rudra N. Sahoo, Malika Kaushik, **Arshiya Sood et al.**
   Proceedings of the DAE Symposium on Nuclear Physics 62, 590 (2017)

3. **Low background radiation measurement at IIT Ropar.**
   I. Ahmed, Vijay Kumar, **Arshiya Sood et al.**
   Proceedings of the DAE Symposium on Nuclear Physics 62, 1078 (2017)

4. **Barrier distribution for $^{16}O + ^{169}Tm$ system through quasi-elastic back-scattering.**
   Abhishek Yadav with **Arshiya Sood** et al.
   Proceedings of the DAE Symposium on Nuclear Physics 62, 670 (2017)

5. **Effect of coupling on sub-barrier fusion: The case of 37 Cl+ 130 Te system.**
   Rudra N. Sahoo, Malika Kaushik, **Arshiya Sood** et al.
   Proceedings of the DAE Symposium on Nuclear Physics 63, 492 (2018)

6. **Role of target deformation in incomplete fusion at energies ≈ 4-7 MeV/A.**
   Unnati Gupta with **Arshiya Sood** et al.
   Proceedings of the DAE Symposium on Nuclear Physics 63, 690 (2018)

7. **Fission fragment angular distribution measurements for the $^{28}Si + ^{180}Hf$ reaction.**
   A. C. Visakh with **Arshiya Sood** et al.
   Proceedings of the DAE Symposium on Nuclear Physics 63, 612 (2018)

8. **Study of quasi-elastic backscattering in $^{7}Li + ^{116,118}Sn$ systems.**
   Arshiya Sood et al.
   Proceedings of the DAE Symposium on Nuclear Physics 64, 333 (2019)

9. **Incomplete fusion studies in $^{14}N + ^{175}Lu$ system.**
   Ishfaq Majeed with **Arshiya Sood et al.**
   Proceedings of the DAE Symposium on Nuclear Physics 64, 331 (2019)

10. **Observation of partial linear momentum transfer in incomplete fusion reactions: A study relevant to non α-cluster beam.**
    Mohd. Shuaib with **Arshiya Sood et al.**
    Proceedings of the DAE Symposium on Nuclear Physics 64, 425 (2019)

11. **Examining the Role of Transfer in Sub-barrier Fusion Enhancement: $^{35,37}Cl + ^{130}Te$ Systems**
    Rudra N. Sahoo, Malika Kaushik, **Arshiya Sood et al.**
    JPS Conf. Proc. 32, 010016 (2020)

12. **Anomalous fragment angular distributions in the fission of composite systems formed in 28,30Si+ 180Hf Reactions**
    R.Murali **with Arshiya Sood et al.**
    Proceedings of the DAE Symposium on Nuclear Physics 65, 213 (2021)

13. **Decay studies in the A∼225 Po-Fr region from the DESPEC campaign at GSI in 2021.**
    M. Polettini with **Arshiya Sood et al.**
    Nuovo cimento c-colloquia and communications in physics 45, 125 (2022)

COLLABORATIVE EXPERIMENTS

Experiments at IUAC, New Delhi , India.

- **Experiment 60205:** ***A study of heavy-ion induced fusion reactions at low energies***
  Spokesperson: Mohd. Shuaib (AMU, Aligarh)
  (June 08-13, 2018)
- **Experiment 58205:** ***Probing of (Multi-) Nucleon-Transfer Events Around the Barrier***
  Spokesperson: Rudra N. Sahoo (IIT Ropar, Punjab)
  (February 13-16, 2018)
- **Experiment 58140:** ***Probing of Heavy Ion Interactions using 19F Beam @ Energy 4-7 MeV/A***
  Spokesperson: Unnati (University of Delhi, Delhi)
  (February 10-12, 2018)
- **Experiment 58205:** ***Probing of (Multi-) Nucleon-Transfer Events Around the Barrier***
  Spokesperson: Rudra N. Sahoo (IIT Ropar, Punjab)
  (December 21-27, 2017)
- **Experiment 61124:** ***Coulomb excitation of 45Sc***
  Spokesperson: M. Matejska-Minda (HIL University of Warsaw, Poland)
  (November 11-30, 2017)
- **Experiment 59404:** ***Measurement of Fusion Barriers for cold and hot fusion reactors***
  Spokesperson: Gurpreet Kaur (PU Chandigarh, Punjab)
  (August 23-29, 2017)
- **Experiment 59211:** ***Investigating the dynamics of heavy ion induced fusion-fission reactions at energies near and above the coulomb barrier***
  Spokesperson: A. Shamlath (CU Kerala, Kerala)
  (August 16-22, 2017)
- **Experiment 59218:** ***Searching the stabilizing effect of N=126 in compound systems formed in heavy ion collision***
  Spokesperson: P. V. Laveen (CU Kerala, Kerala)
  (August 08-14, 2017)
- **Experiment 58129 :** ***Influence of Hexadecapole Deformation on Heavy-Ion Reaction Mechanism***
  Spokesperson: Abhishek Yadav (IUAC, New Delhi)
  (January 09-14, 2017)

COLLABORATIVE EXPERIMENTS

Nuclear Physics DESPEC FAIR phase-0 experiment campaign at GSI, Darmstadt, Germany.

- **Experiment S452:** ***The Prolate-Oblate Shape Transition around A~ 190***
  Spokesperson: Philip R. John (TU, Darmstadt) and P. Koseoglou (TU, Darmstadt)
  (March 05-15, 2021)

- **Experiment S460:** ***Investigation of 220>A>230 Po-Fr nuclei lying in the south-east frontier of the A~225 island of octupole deformation***
  Spokesperson: G. Benzoni (INFN, Milano) and JJ Valiente Dobon (INFN-LNL, Legnaro)
  (April 15-23, 2021)

- **Experiment S496:** ***Core-breaking in the most neutron-deficient Tin isotopes***
  Spokesperson: G. Zhang (INFN, Padova) and D. Mengoni (INFN, Padova)
  (May 11-22, 2021)

JUROGAM3-MARA campaign at the JYFL Accelerator Laboratory, Jyväskylä, Finland.

- **Experiment JM09:** ***Search for the isoscalar spin-aligned pairing scheme in self-conjugate 96Cd***
  Spokesperson: Bo Cederwall (KTH, Stockholm) and B. S. Nara Singh (University of Manchester, UK)
  (October 25-31, 2021)

- **Experiment JM41:** ***Identification of excited states in 78Zr***
  Spokesperson: D. Jenkins (University of York, UK)
  (November 01-04, 2021)

Thank you!

QUASI-ELASTIC BACKSCATTERING IN ^{7}Li+ ^{116,118}Sn SYSTEMS

EVENT SELECTION

- ***To select events of interest in Z=3 band, Q-value spectra for Z=3 events were calculated using kinematical relation***

$$Q = \left(\frac{A_t + A_p}{A_t}\right) E_2 - \left(\frac{A_t - A_p}{A_t}\right) E_1 - \left(\frac{2A_p\sqrt{E_1 E_2}}{A_t}\right) \cos\theta,$$

where θ is the scattering angle in the laboratory frame. A_t and A_p are the mass numbers for projectile and target, respectively. E_1 is the energy loss corrected incoming energy of the projectile before scattering and E_2 is the energy of the projectile after scattering at angle θ.

- ***For events of interest for Z=2 band, the widths of α-particle yield were calculated using relation***

$$E^{max}_{min}(\alpha) = E\left(\frac{m_\alpha}{M}\right)\left(1 + \frac{E_x}{E}\frac{m}{m_\alpha} \pm 2\sqrt{\frac{E_x}{E}\frac{m}{m_\alpha}}\right)$$

where $E^{max}_{min}(\alpha)$ are the minimum and maximum laboratory energies of the α particle, E is the energy of ^{7}Li scattered to angle θ, E_x is the excitation energy of $\alpha + x$ system above threshold and m_α=4, M=7 and m=x (x depends on the breakup channel). For instance, from Eq. 4.5, the maximum and minimum energy of alpha

Q values of different reaction channels

^{7}Li+^{116}Sn Reaction channel	Q_{gg} (MeV)	^{7}Li+^{118}Sn Reaction channel	Q_{gg} (MeV)
^{116}Sn(^{7}Li,^{5}Li)^{118}Sn	3.355	^{118}Sn(^{7}Li,^{5}Li)^{120}Sn	2.673
^{116}Sn(^{7}Li,^{6}Li)^{117}Sn	-0.308	^{118}Sn(^{7}Li,^{6}Li)^{119}Sn	-0.768
^{116}Sn(^{7}Li,^{8}Li)^{115}Sn	-7.531	^{118}Sn(^{7}Li,^{8}Li)^{117}Sn	-7.293
^{116}Sn(^{7}Li,^{6}He)^{117}Sb	-5.571	^{118}Sn(^{7}Li,^{6}He)^{119}Sb	-4.863
^{116}Sn(^{7}Li,^{8}Be)^{115}In	7.976	^{118}Sn(^{7}Li,^{8}Be)^{117}In	7.256
^{116}Sn(^{7}Li,^{3}H)^{120}Te	-2.201	^{118}Sn(^{7}Li,^{3}H)^{121}Sb	-1.381
^{116}Sn(^{7}Li,^{4}He)^{119}Sb	10.430	^{118}Sn(^{7}Li,^{4}He)^{121}Sb	10.428
^{116}Sn(^{7}Li,^{5}He)^{119}Sb	-0.009	^{118}Sn(^{7}Li,^{5}He)^{120}Sb	0.286

- **Q-value spectra were integrated over the window (-1,3.3) MeV depending on θ_{lab} and E_{lab}**
- **elastic and inelastic scattering events and some contributions from 1n , 2n stripping reactions**

- **Inclusive α measurements – contribution from direct or sequential, no capture and transfer-triggered breakup**
- **Widths of ~ 8-13 MeV are considered for analysis, depending on different projectile energies.**
- **No contribution from evaporation alphas and/or residual (C, O or N) contamination was observed – peaks below 6 MeV.**

cross-sections for

- **"elastic+inelastic" channels are obtained from the selected region in Z=3 band.**
- **"elastic+inelastic+alpha" channels are obtained by adding alpha yield (Z=2 band) to "elastic+inelastic" cross-sections.**

Post-doc Research Summary

STUDY OF β-DELAYED PROTON DECAY OF ^{96}Ag AT THE GSI-FAIR FACILITY

Motivation

- Several research topics in nuclear structure and astrophysics converge on and around the heaviest doubly magic nucleus ^{100}Sn
- Experimental $T_{1/2}$ and $b_{\beta p}$ are needed for reaction flow calculations of the rp capture process of nucleosynthesis.
- Current experimental knowledge of mass, structure and decay properties of nuclei in N?Z region is not exhaustive.
- Improved precision and production rates of these exotic nuclei at different accelerator facilities enabled a more detailed investigation.
- β-decay of ^{96}Ag is particularly interesting as it populates neutron magic (N=50) nuclei ^{96}Pd and ^{95}Ru through $\beta\gamma$ and βp emissions, respectively.

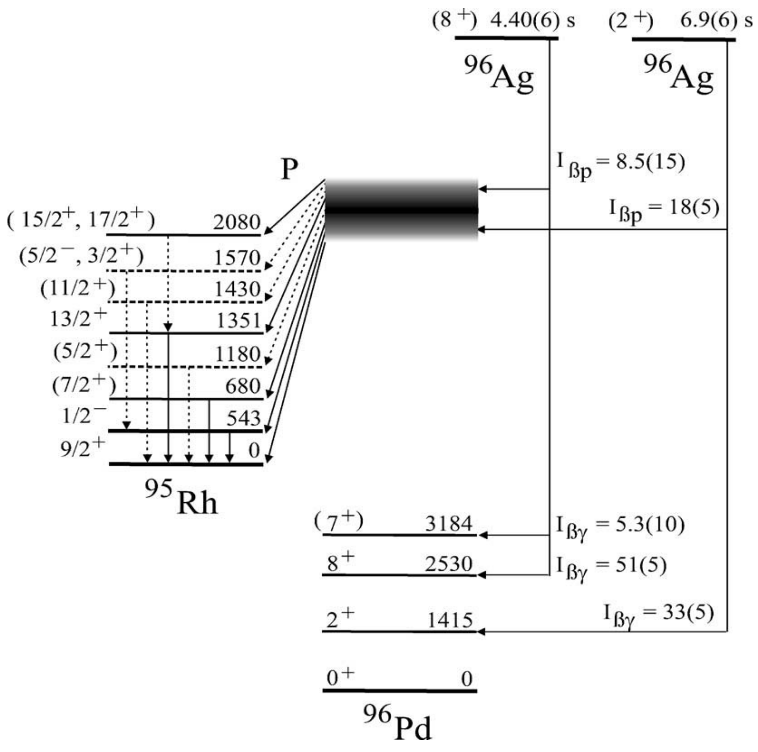

L. Batist et al., Nucl. Phys. A 720, 245 (2003)

S480 Physics commissioning - first new physics experiment for DESPEC @ FAIR0 (March 2020)

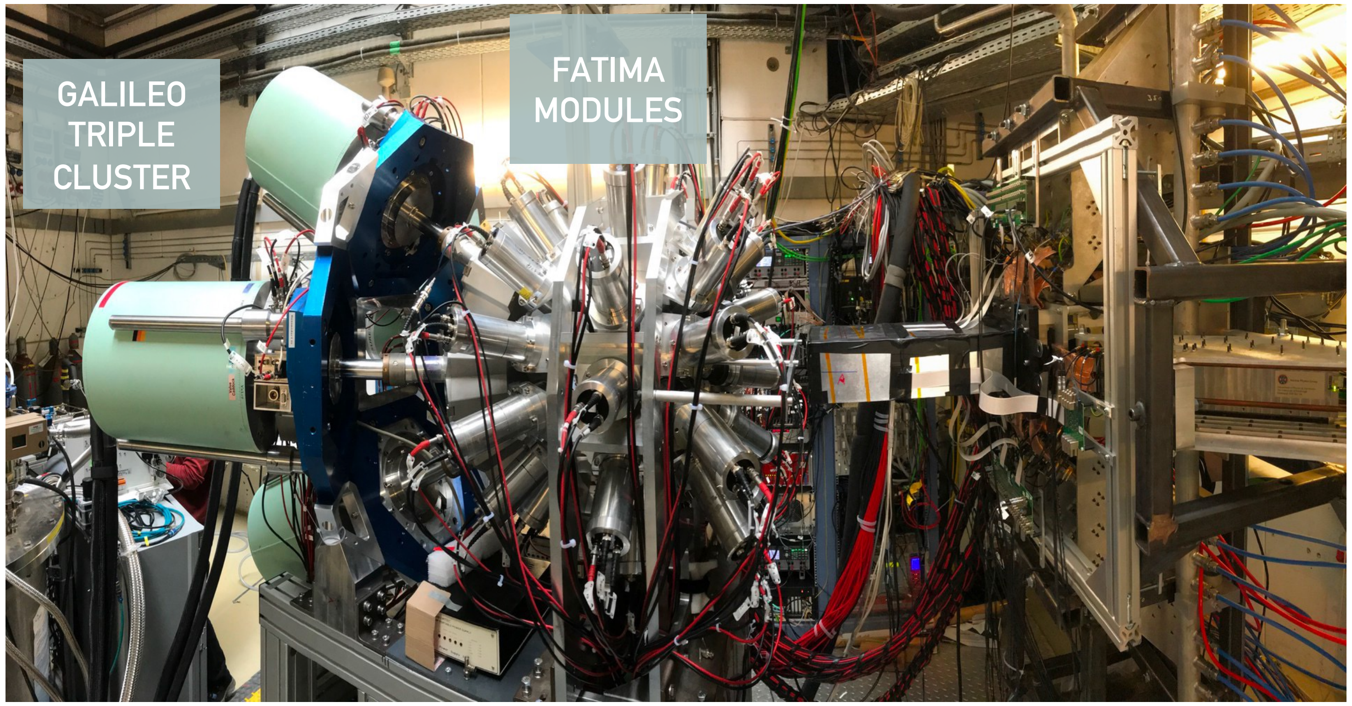

- Fragmentation of ^{124}Xe beam on ^{9}Be target @ 850 Mev/u
- AIDA Implantation array : 3 highly segmented DSSD layers
- AIDA sandwiched by 2 β-Plasts : plastic scintillators
- 36 FATIMA $LaBr_3$ (Ce) detectors
- 6 GALILEO HPGe triple cluster detectors
- New EDAQ

STUDY OF β-DELAYED PROTON DECAY OF ^{96}Ag AT THE GSI-FAIR FACILITY

Experimental Set-up

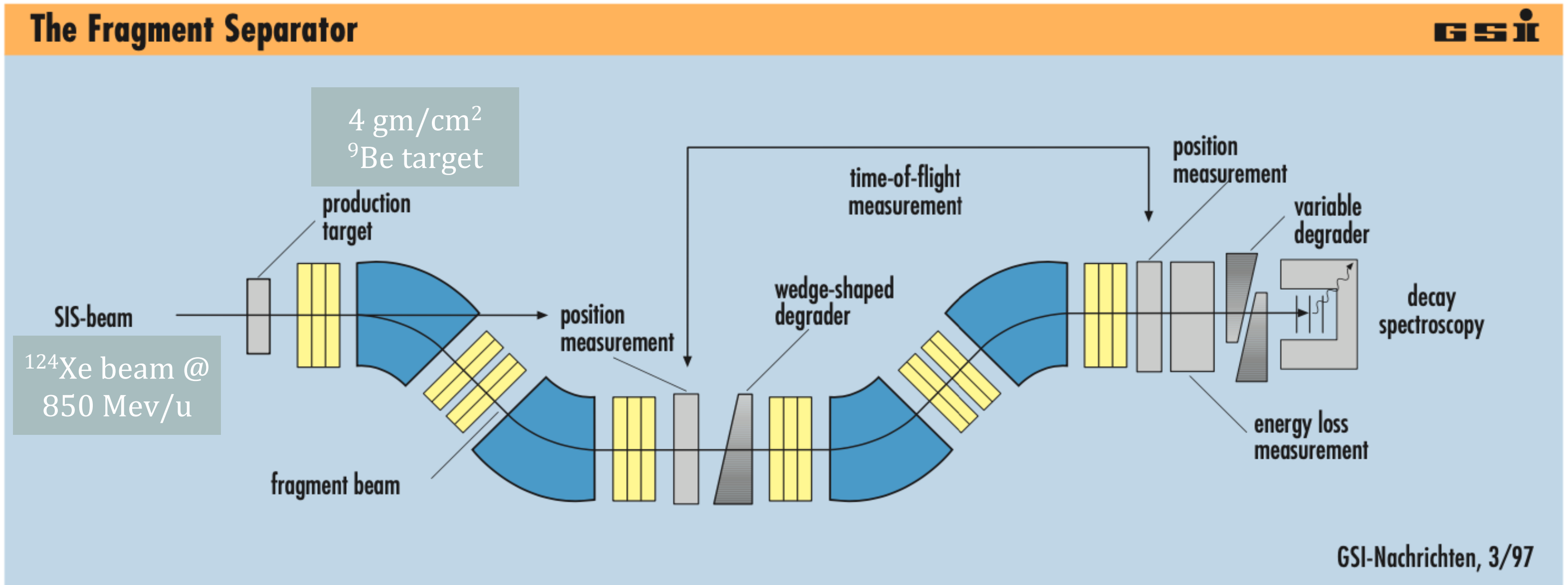

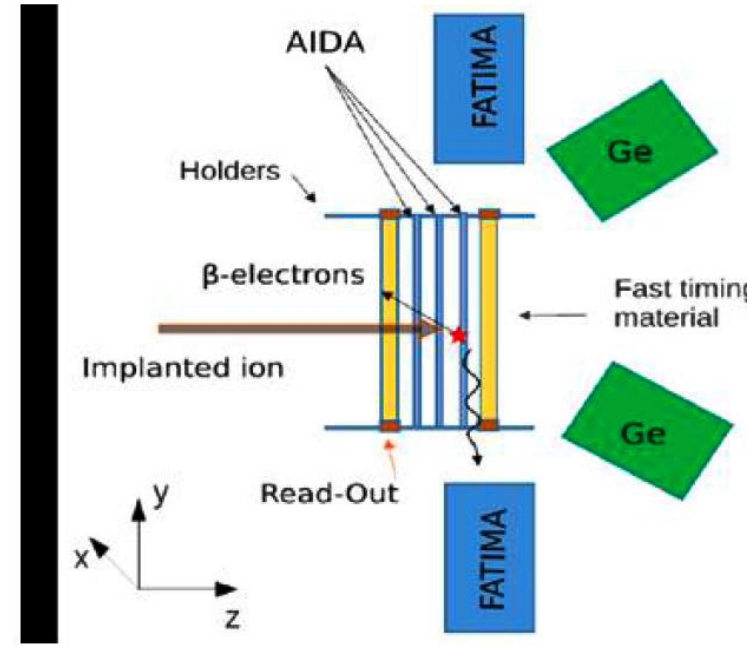

Implantation map : ^{96}Ag

FRS - Z vs A/Q

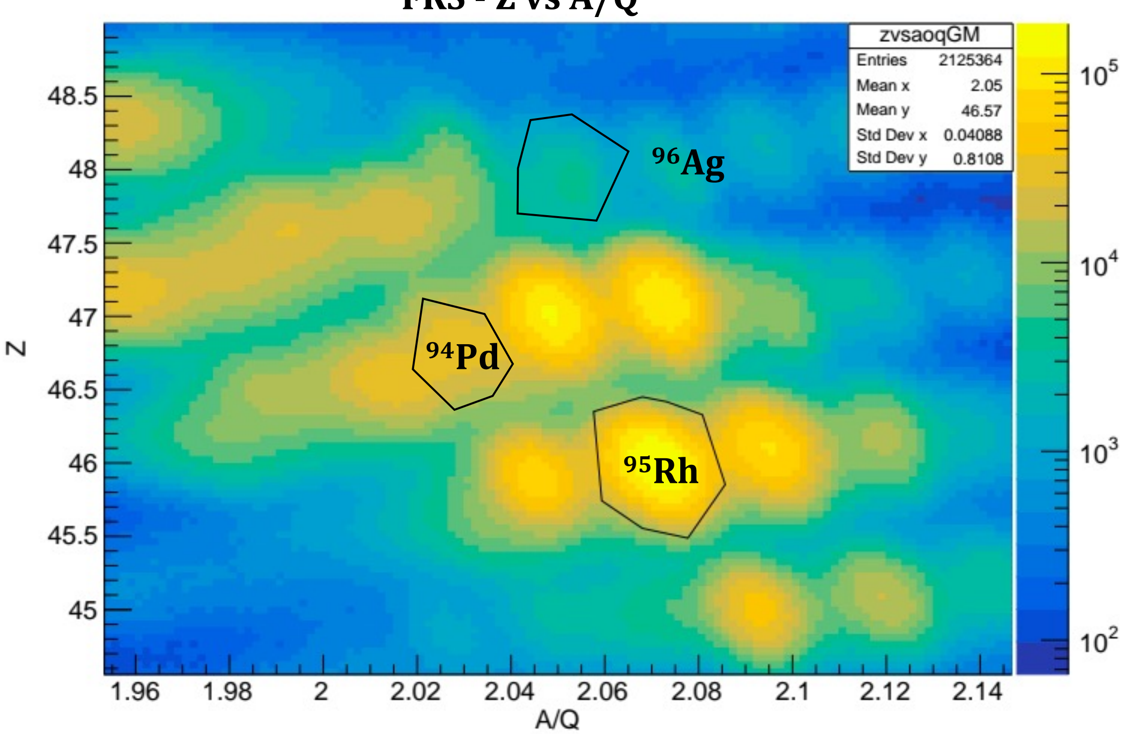

^{96}Ag ions from FRS are implanted on the AIDA

Implantation on DSSD2

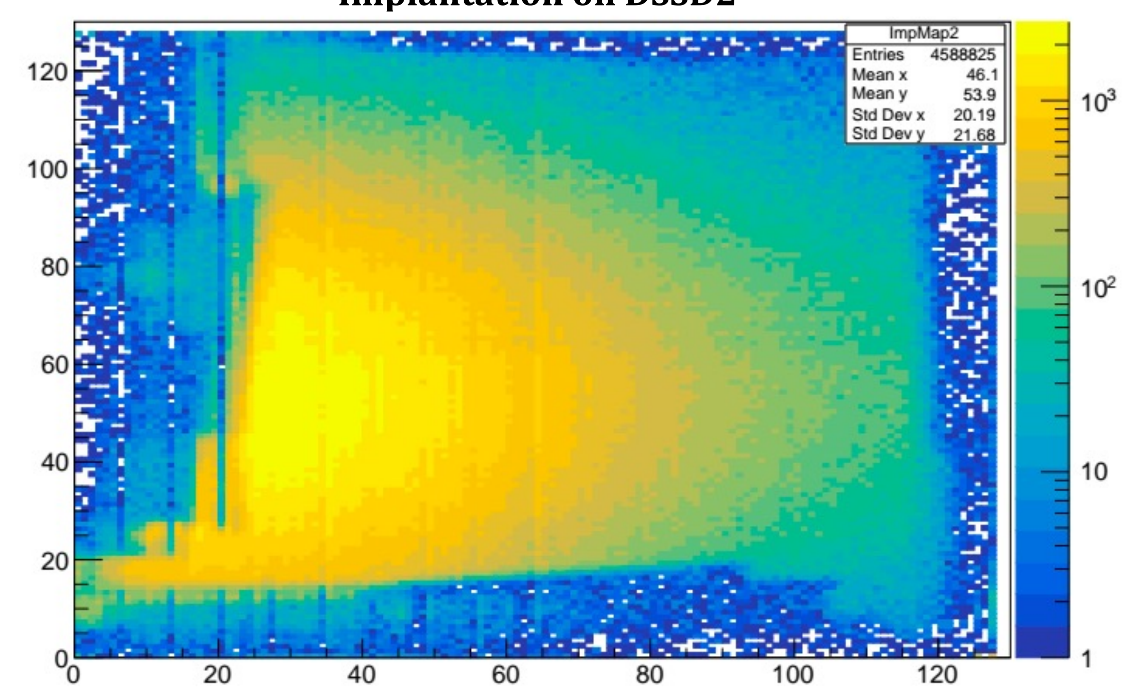

Implant timing is stored as a function of position $T_{implant}(x,y)$

STUDY OF β-DELAYED PROTON DECAY OF ^{96}Ag AT THE GSI-FAIR FACILITY

β- decay at DSSD

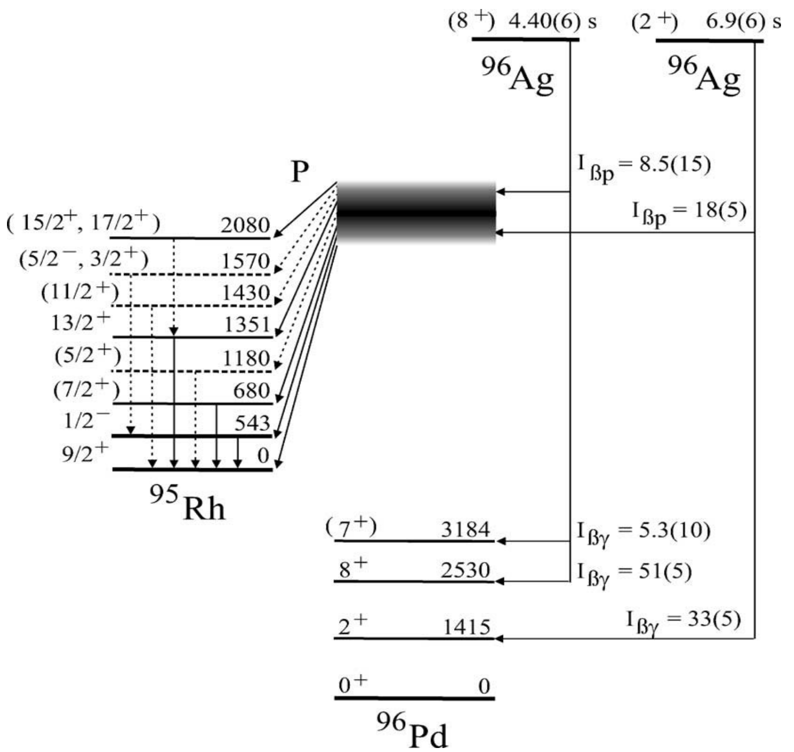

To be measured using β-γ-γ and βp-γ-γ coincidences

White Rabbit Time Correlation

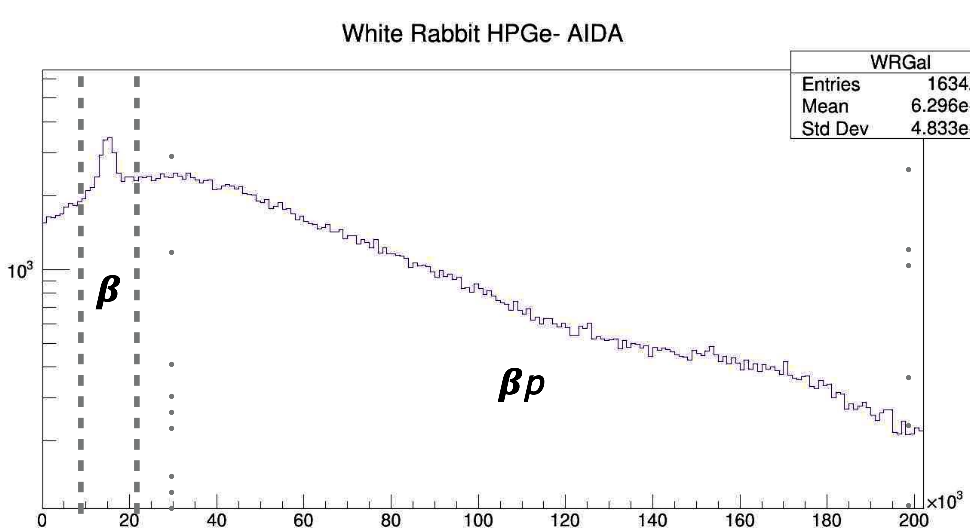

$$T_{implant}(x,y) < T_{decay}(x,y) < T_{implant}(x,y) + 3\tau_{1/2}$$

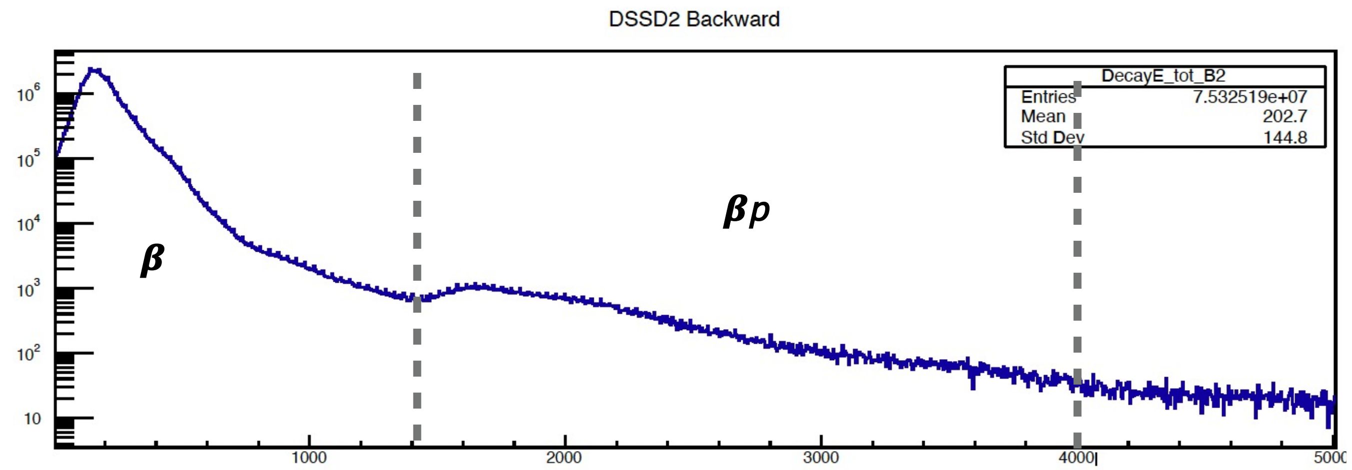

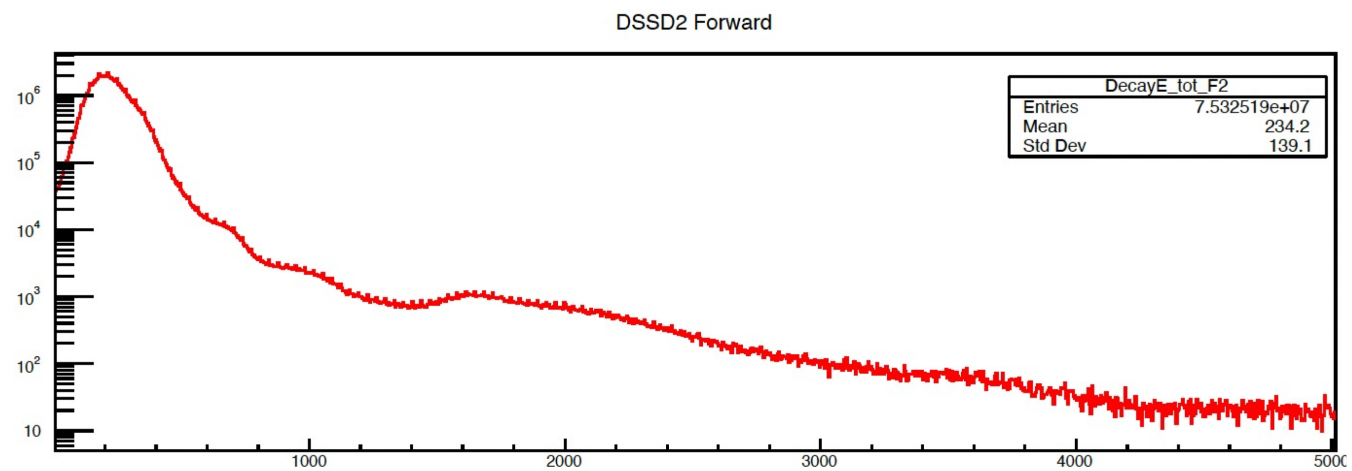

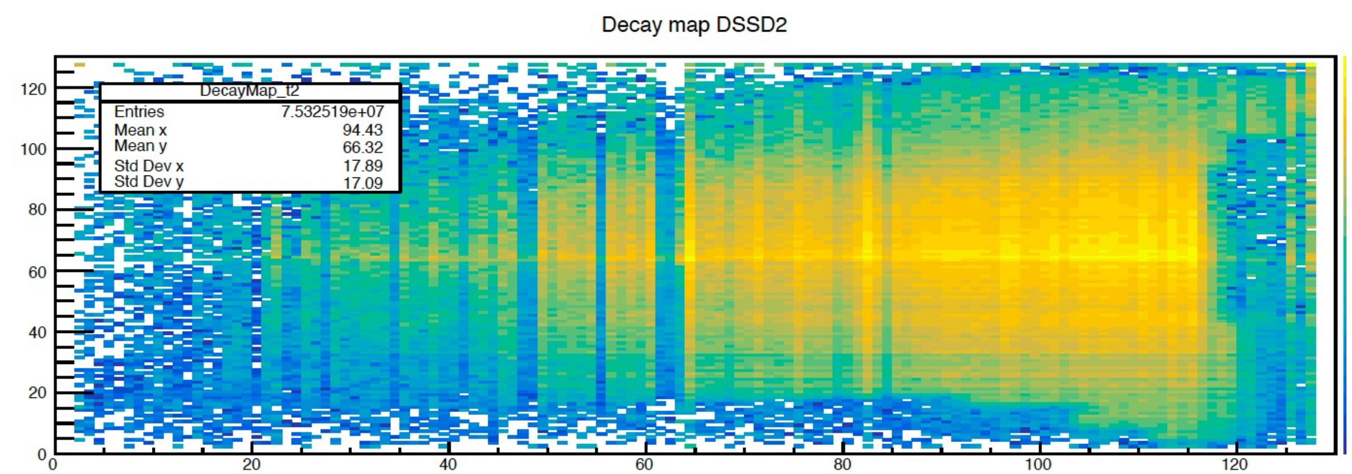

STUDY OF β-DELAYED PROTON DECAY OF ^{96}Ag AT THE GSI-FAIR FACILITY

The HPGe Energy spectra

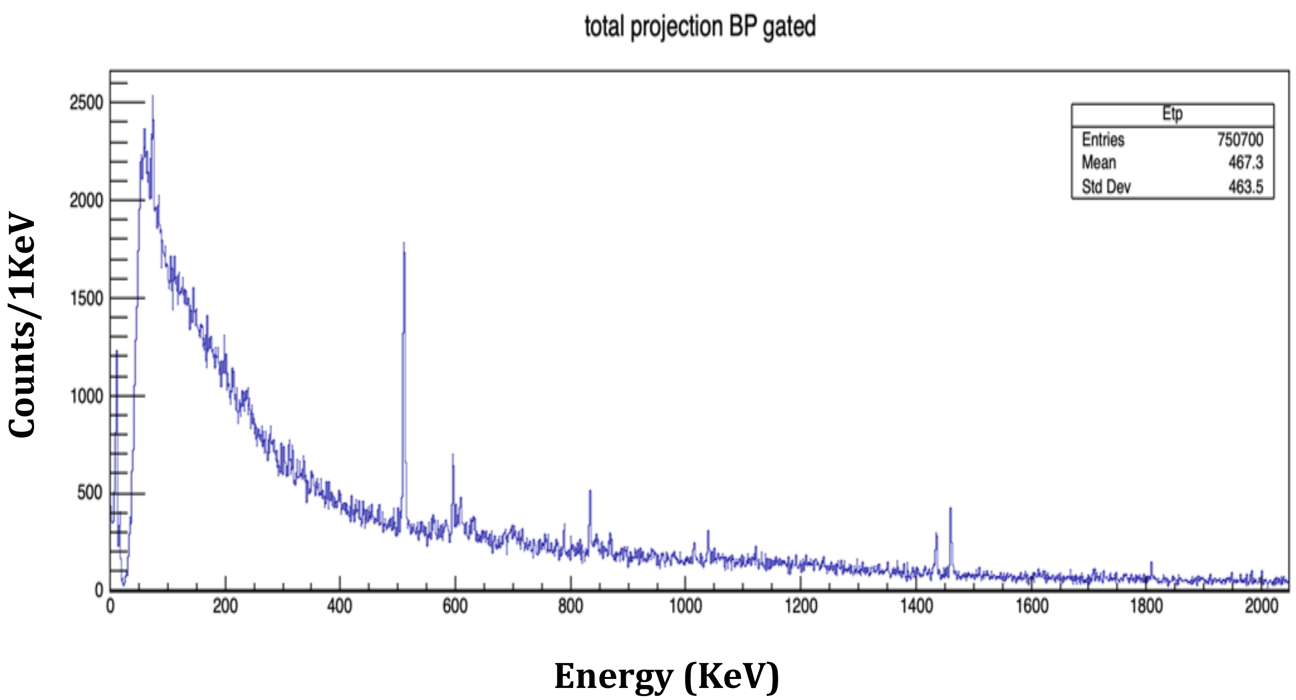

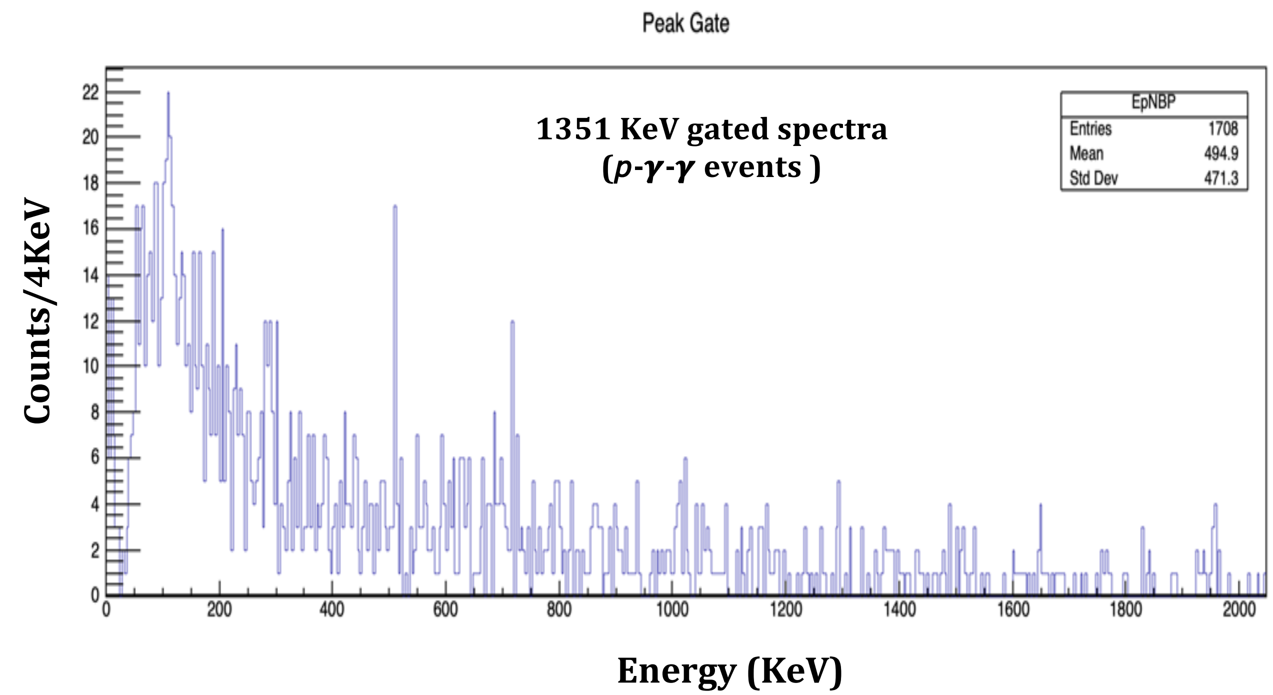

MARA+JUROGAM3+UoYtube campaign at JYFL, Finland

JM09 : Search for the isoscalar spin-aligned pairing scheme in self-conjugate 96Cd

- **Experimental identification of the lowest excited states in 96Cd is needed in order to firmly establish the isoscalar spin-aligned pairing scheme in these nuclei**
- **Fusion evaporation : ^{40}Ca(^{58}Ni,2n)^{96}Cd reaction at a beam energy of 230 MeV close to the Coulomb barrier**
- **Estimated cross-section is 0.5 µb out of a total cross-section of ~40mb for A=96 residues (HIVAP).**
- **Channel selection for the rare 96Cd events was performed by a combination of A/q identification in MARA and recoil-β tagging using plastic scintillators.**
- **UoYtube charged particle detector were employed for rejection of events from fusion evaporation reactions products - 96Ag (pn) and 96Pd (2p - 99% of A=96 isobars)**
- **Gamma-rays from isomeric decays at the MARA focal plane were observed using the clover germanium detectors (JUROGAM3) placed in close configuration - prompt**

Experimental setup